Engineering 59 (2026) 178–196

Contents lists available at ScienceDirect

Engineering

journal homepage: www.elsevier.com/locate/eng

Research
Low Carbon Transformation for Conventional Energies—Article

A Novel Coal Purification-Combustion Technology: Purification Characteristics and Ultra-Low Nitrogen Combustion at Low Load

Shaobo Yang [a], Shaobo Han [a,b], Ruifang Cui [a,b], Linxuan Li [a,b], Chen Liang [a], Shuai Guo [a], Neng Fang [a], Wei Li [a,b], Qiangqiang Ren [a,b,*]

[a] State Key Laboratory of Coal Conversion, Institute of Engineering Thermophysics, Chinese Academy of Sciences, Beijing 100190, China
[b] University of Chinese Academy of Sciences, Beijing 100049, China

ARTICLE INFO

Article history:
Received 19 March 2025
Revised 15 September 2025
Accepted 25 September 2025
Available online 15 October 2025

Keywords:
Low load
High temperature purification
Moderate or intense low-oxygen dilution combustion
Nitrogen migration
Ultra-low nitrogen emission

ABSTRACT

To meet the demand for clean and efficient coal utilization under low-load conditions and new power systems, an innovative coal purification-combustion technology is proposed in this study. The feasibility and fuel adaptability were verified using a 200 kW coal purification-combustion system. The high-temperature purification characteristics of three types of coal under a low load of 55% and the nitrogen migration and transformation mechanism during the purification-combustion process were studied. The results show that the medium-temperature activation process mainly involves the release and reduction of volatile nitrogen to N_2, with a nitrogen conversion rate of 43.8%–53.1%. During this process, coal powder activation is achieved, which significantly increases the specific surface area of the char, develops a pore structure, and increases the number of active sites, which are beneficial for high-temperature gasification reactions under low loads. During high-temperature purification, 62%–85% of the inorganic components were separated, achieving the separation of carbon and inorganic components. Coal powder is converted into high-temperature gaseous fuel, mainly composed of CO and H_2, and the pore structure of char is further developed, which is conducive to stable combustion under low loads. The high-temperature purification process mainly involves the release and reduction of char nitrogen to N_2, with a nitrogen conversion rate of 93.6%–96.6%. The fuel, mainly composed of high-temperature CO and H_2, achieved a moderate or intense low-oxygen dilution (MILD) combustion process. In the reduction zone of the combustion furnace, NH_3 was completely converted to N_2 and char nitrogen was gradually released and reduced to N_2, with a nitrogen conversion rate of 99.6% in the reduction zone. The oxidation zone involves the burnout of char, which mainly releases char nitrogen and oxidizes it to NO_x. Ultimately, only 0.2%–0.9% of the coal nitrogen is converted to NO_x. The minimum original NO_x emissions of the three types of coal at low loads were 28 mg·Nm^{-3} (@6% O_2), and the combustion efficiency exceeded 99.6%.

1. Introduction

Currently, the rapid development of renewable energy in China aims to optimize the energy structure, reduce dependence on coal, and reduce CO_2 emissions. However, owing to the intermittency and volatility of renewable energy, it is challenging to achieve the stable power output required for electricity generation. Therefore, clean and efficient combustion of coal remains crucial. Power station boilers must operate under a wide load range, particularly at low loads, facing issues of incomplete coal combustion and high pollutant emissions at low loads.

The primary condition for achieving clean and efficient coal combustion under low loads is to improve the combustion efficiency of pulverized coal [1]. The combustion efficiency of pulverized coal is mainly related to factors such as the coal type, combustion temperature, reaction atmosphere, and reaction time. Higher volatile coal types, higher combustion temperatures, oxygen-rich reaction atmospheres, and longer reaction times are conducive to improving combustion efficiency [2–4]. The development of high-efficiency combustion technologies with broad adaptability to various reaction conditions is crucial. Clean coal combustion mainly focuses on the emissions of combustion

* Corresponding author.
E-mail address: renqiangqiang@iet.cn (Q. Ren).

https://doi.org/10.1016/j.eng.2025.09.026

pollutants. Owing to the unstable chemical properties and complex transformation mechanisms of NO_x, it is difficult to effectively control during combustion, and the issue of increased NO_x emissions at low loads is particularly prominent [5]. At reduced loads, combustion becomes unstable, which promotes the formation of localized high-temperature, oxygen-rich zones, which enhance NO_x formation. Moreover, frequent load fluctuations under low operating conditions, combined with delayed adjustments of air and coal flow, lead to significant variations in the oxygen concentration and temperature fields. As a result, NO_x emissions exhibit substantial variability and remain at elevated levels [6]. In recent years, reducing NO_x emissions during coal combustion under low loads has become a research hotspot. Technologies, such as low-NO_x burners and staged combustion, have been proposed [7–9]. However, these conventional technologies reportedly control the initial NO_x emissions to approximately 200–500 $mg{\cdot}m^{-3}$, but at the cost of combustion efficiency, making it difficult to achieve clean and efficient coal utilization under low load. Therefore, it is necessary to explore new clean and efficient coal-combustion technologies [10,11].

The Institute of Engineering Thermophysics, Chinese Academy of Sciences, has developed a preheated combustion technology for pulverized coal. This technology has advantages such as strong fuel adaptability, high combustion efficiency, low NO_x emissions, and flexible load adjustment [12]. Compared with traditional coal combustion methods, most volatile nitrogen and part of the char nitrogen in coal are released into the gas phase during preheated combustion. Under a strongly reducing atmosphere, most of it is converted to N_2, and a small amount is converted to nitrogen-containing intermediates (HCN, NH_3), thereby reducing the generation of NO_x during combustion. The preheated fuel enters the combustion chamber. Through reasonable air distribution, the gas–solid mixing intensity and combustion temperature are controlled, achieving high-efficiency combustion and low NO_x emissions. This technology has been verified on a 30 kW pilot test bench and a 2 MW pilot test bench. Reducing the particle size distribution of raw coal, increasing the primary air equivalent ratio (ER), increasing the preheating temperature, and increasing the oxygen concentration are all conducive to increasing the effective gas components of the preheated coal and improving the reactivity of the char [13,14]. By optimizing operating conditions, the ultra-low NO_x emission level during the preheating process can be reduced to below 50 $mg{\cdot}m^{-3}$ (@6% O_2), but at the cost of combustion efficiency [15,16]. However, despite extensive research on this technology, the minimum NO_x emissions are still far from the national emission standards. Increasing the temperature of the preheating zone can promote the precipitation of coal nitrogen during the preheating stage, thereby further reducing NO_x emissions. However, due to the structural characteristics of the fluidized bed itself, the preheating temperature of the preheated combustion technology cannot exceed 1000 °C, which limits the precipitation of char nitrogen in coal. Wang et al. [17] further increased the preheating temperature to 1050 °C and conducted wide-load experimental studies, showing that increasing the preheating temperature can improve the precipitation and reduction of coal nitrogen during the preheating process, achieving NO_x emissions of around 120 $mg{\cdot}m^{-3}$ under a wide load range of 45–75 kW.

To further break through the original NO_x emission values of coal combustion under low load and achieve efficient ultra-low nitrogen combustion under low load, the Institute of Engineering Thermophysics, Chinese Academy of Sciences, proposed a new coal purification-combustion technology (Fig. 1) [18–20]. By constructing a thermal coal purification system, the complex components of coal are separated through high-temperature purification (150 °C above the flow temperature (FT)), achieving directional conversion and removal of N and inorganic components, completing the purification process of coal. This process removes impurities during coal combustion, transforming coal into clean carbon fuel mainly composed of CO, changing the fuel properties of coal to raw material properties. The purification of coal changes the traditional combustion reaction path of coal, achieving a transition from heterogeneous reaction-dominated to homogeneous reaction-dominated coal combustion. This significantly improves the combustion reaction rate of carbon fuel, meeting the needs of flexible coal-fired power generation in new power systems dominated by new energy. Su et al. [21,22] completed the preliminary verification of this technology based on a 30 kW pilot device, studying the influence of factors such as air distribution structure and furnace type, achieving NO_x emissions of 39.5 $mg{\cdot}m^{-3}$ and a combustion efficiency of 99.3%. However, the maximum purification temperature of this device is only 1100 °C, making it impossible to further reduce NO_x emissions. Han et al. [20] conducted preliminary studies on the NO_x emission characteristics of coal under wide load conditions on a 200 kW purification-combustion system, achieving stable operation of purification-combustion under a wide load range of 50%–100%, with NO_x emissions reaching around 50 $mg{\cdot}m^{-3}$ under low load, demonstrating the potential of purification-combustion technology to further reduce NO_x emissions.

In this study, purification (> 1300 °C) combustion experiments of multiple coal types under low loads were conducted on a 200 kW coal purification-combustion system. The high-temperature gasification reaction, moderate or intense low-oxygen dilution (MILD) combustion organization, and nitrogen migration and transformation mechanisms during the purification-combustion process were thoroughly investigated. Ultimately, efficient ultralow nitrogen combustion of multiple coal types under low load was achieved, verifying the advantages of coal purification-combustion technology.

2. Experimental and material

2.1. Experimental system

The process flow of the 200 kW coal purification-combustion system is shown in Fig. 2. The system mainly consisted of a medium-temperature activation unit (MT), a high-temperature purification unit (HT), mild combustion unit (SC), and other auxiliary systems. The MT comprises two circulating fluidized beds, each with an inner diameter of 110 mm and height of 1500 mm. During the experiment, the parameters of the two circulating fluidized beds were kept consistent to ensure a uniform operation. In MT, the fuel mixed with primary air undergoes pyrolysis, gasification, and combustion reactions. The fuel was preheated to approximately 850 °C, and the resulting char and coal gas were introduced into the HT through opposing burners along with secondary air. The HT furnace had an inner diameter of 300 mm and height of 1000 mm, with the opposed burners located 300 mm above the furnace bottom. Under the action of opposed burners, the gas–solid composite fuel produced by the circulating fluidized beds of the MT rapidly burns upon contact with the secondary air, forming a core high-temperature zone and undergoing a purification process. During this process, the carbon–hydrogen components of the fuel are further consumed and converted into high-quality coal gas, while the inorganic components partially form liquid slag, which is captured and flows into the quenching pool for water cooling and discharge. The high-temperature coal gas produced by the HT-carrying char, flowed upward into the SC. Therefore, the purpose of MT is to modify coal and provide high-temperature gas–solid materials for HT.

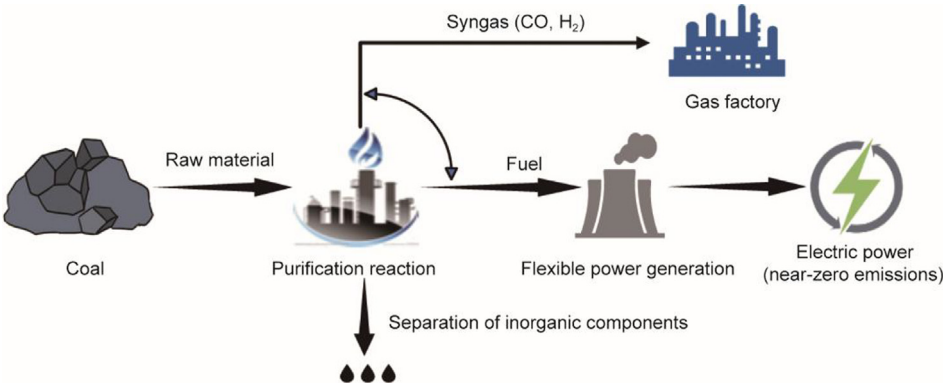

Fig. 1. The concept of coal purification-combustion.

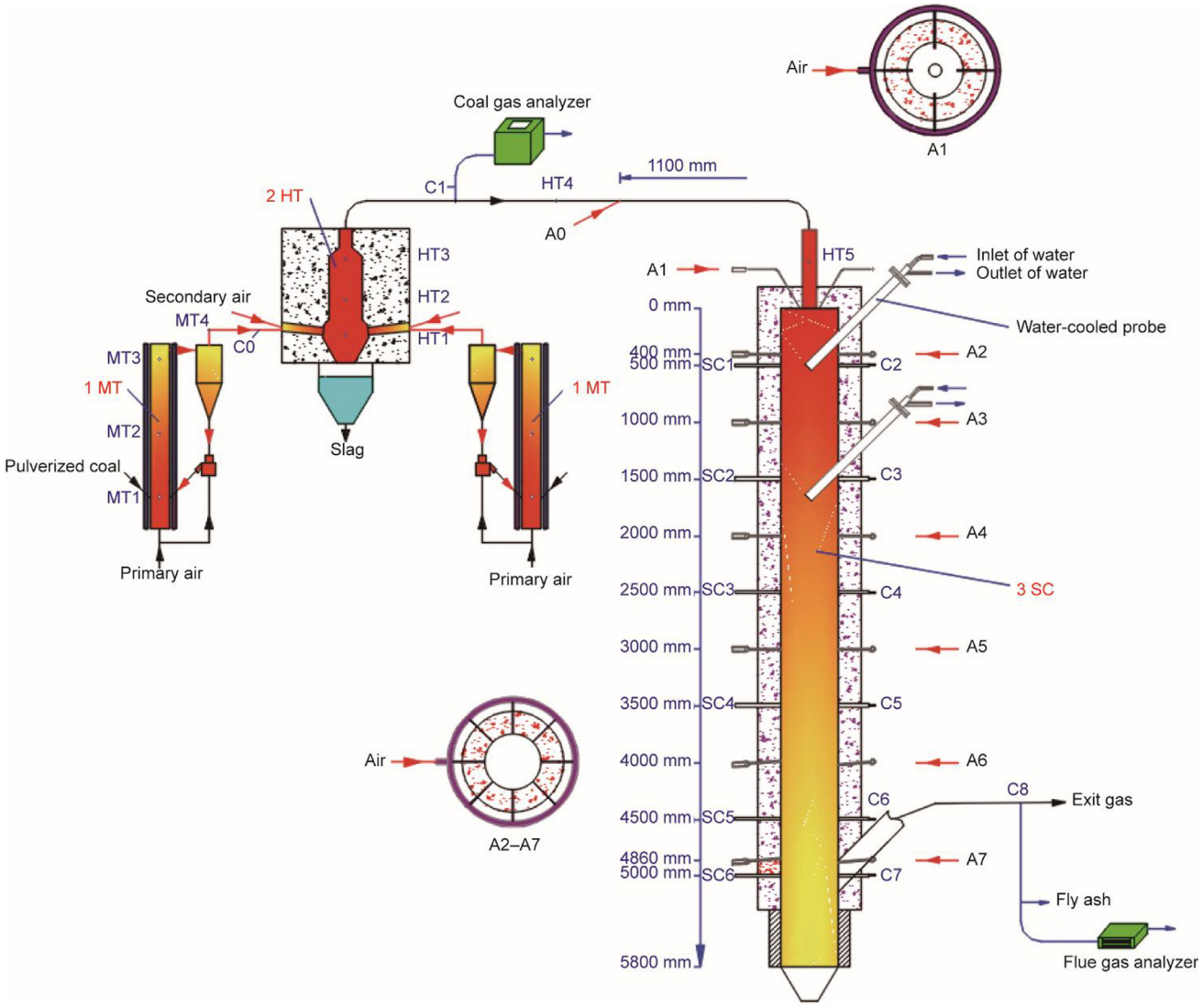

Fig. 2. Process flow of the 200 kW coal purification-combustion system.

The SC furnace had an inner diameter of 500 mm and height of 5000 mm, with tertiary air divided into A1–A7 levels entering the furnace. The high-temperature hot fuel from the HT furnace outlet underwent slow and mild combustion in the SC furnace under the A1–A7 level air distribution. At the entrance of the SC, swirl fins are set up to make the hot gas swirl into the SC, thereby enhancing disturbance and mixing. The A1 level air distribution consisted of four evenly arranged ring nozzles, with each nozzle introducing air into the furnace at a 30° to the hot fuel. The A2–A5 level air distributions each consisted of eight evenly arranged ring nozzles, with each nozzle introducing air horizontally into the furnace, perpendicular to the flow of the hot fuel. The purpose of such a setting is to enhance disturbance, thereby intensifying the release of char nitrogen and its reduction to N_2. The A6 and A7 level air

distributions also consist of eight evenly arranged ring nozzles, but unlike the A2–A5 level nozzles, the nozzles in the A6 and A7 levels are symmetrically arranged with four nozzles angled 5° upward and four nozzles angled 5° downward. The purpose of this setting is to reduce the combustion intensity, thereby suppressing the conversion of char nitrogen to NO_x in the oxidation zone. The hot fuel from the HT outlet gradually burned out in the SC, and flue gas was discharged from the bottom of the SC furnace. Two-stage water-cooled probe-heating surfaces were arranged at the furnace inlet to prevent excessively high combustion temperatures.

Three K-type thermocouples were arranged along the riser of each MT circulating fluidized bed, designated as MT1–MT3, with one K-type thermocouple at the outlet, designated as MT4. Three B-type thermocouples were arranged along the HT furnace, designated as HT1–HT3, with two S-type thermocouples arranged along the HT outlet flue gas channel, designated as HT4 and HT5. Six S-type thermocouples were arranged along the SC furnace, designated as SC1–SC6. The coal gas and char produced in the MT and HT were sampled at points C0 and C1, respectively, whereas the coal gas and char along the SC furnace were sampled at points C2–C7. The fly ash and flue gas components from the combustion were sampled at point C8 in the flue. The coal gas components during the process were analyzed online using a gas analyzer (TY-6030P), and the flue gas components were measured online using a Testo flue gas analyzer (Testo350). Fly ash was collected during the process using a vacuum pump. The nitrogen-containing gas-phase components (HCN, NH_3, and NO_x) during the reaction process were measured using portable detection tubes (KIT-AGAWA) at points C0–C7.

2.2. Experimental materials

Three types of coal were selected as the raw materials for the experiment: Shenmu bituminous coal (SM), Beishan lignite (BS), and Yihua coal (YH), with particle sizes ranging from 0 to 0.18 mm. The fuel characteristics are listed in Table 1. The FT of all three coals were below 1250 °C, making them suitable for liquid slagging. The proximate analysis results of the test coal were measured in accordance with the provisions of "GB/T 212–2008 Method for Proximate Analysis of Coal," while the ultimate analysis results were obtained through analysis and measurement using an organic elemental analyzer experimental instrument.

2.3. Experimental conditions

The experimental conditions are listed in Table 2. The experiment was conducted at a low load of ~55%. During this process, the thermal load, MT ER (λ_1), HT ER (λ_2), SC ER (λ_3), and total ER (λ_T) were maintained constant for the three coals. Here, λ_P represents the ER of purification system, which is the sum of λ_1 and λ_2. The operating temperatures for the MT and HT stages were determined through comprehensive optimization, balancing the reaction effectiveness and system stability. The MT temperature was set at approximately (850 ± 30) °C to maximize volatile release and char modification, while avoiding slagging and instability. For HT, the temperature was defined as exceeding the FT of each coal type by at least 150 °C, ensuring effective liquid slag formation, impurity removal, and the conversion of char N to N_2. To ensure comparability and operational stability under low-load conditions, a uniform ER was applied across all coal types. The selected ratios reflect a balance between system stability, inter-sample comparability, and optimal nitrogen reduction performance, as supported by our previous studies on SM coal under varying ERs [23]. The calibration curves for the feeders are shown in Fig. 3.

2.4. Calculation methods

The conversion rate C_X of each component to the gas phase after the pulverized coal reaction was calculated based on the ash balance using the Eq. (1).

$$C_X = (1 - \frac{A_1 \times X_2}{A_2 \times X_1}) \times 100\% \quad (1)$$

where C_X (%) is the conversion rate of coal component X, A_1 (%) and X_1 (%) are the mass fractions of coal ash and component X before the reaction, respectively, and A_2 (%) and X_2 (%) are the mass fractions of ash and component X in the fly ash after the reaction, respectively.

The calculation formulas for the conversion of coal nitrogen to slag nitrogen, char nitrogen, gas-phase nitrogen, and NO_x during the pulverized coal purification-combustion process are presented in Eqs. (2)–(7) of Ref. [23].

The calculation formula of the ash removal rate is as follows:

$$\eta = \frac{m_s \times A_s}{m_0 \times A_1} \times 100\% \quad (2)$$

where η (%) is the ash removal rate, m_s (kg) is the mass of the slag during the working condition, A_s (%) is the ash content of the molten slag, and m_0 (kg) is the total mass of pulverized coal fed into the working condition.

The yields of char at different reaction stages were calculated based on the ash balance using the following formula:

$$y_{c,MT} = A_1/A_2 \quad (3)$$

$$y_{c,HT} = (m_0 \times A_1 - m_s \times A_s)/(m_0 \times A_2) \quad (4)$$

Table 1
Fuel characteristics.

Type	Ultimate analysis (wt%, air dry)					Proximate analysis (wt%, air dry)					Ash fusion temperature (°C)			
	C	H	O	N	S	Moisture	Ash	Volatile matter	Fixed carbon	Low heating value ($MJ·kg^{-1}$)	DT	ST	HT	FT
SM	71.51	3.45	10.21	0.87	0.36	8.12	5.48	31.41	59.26	26.96	1200	1210	1220	1250
BS	59.30	2.57	13.75	0.72	0.30	10.96	12.40	25.44	51.20	21.38	1000	1010	1010	1040
YH	68.87	3.27	13.48	0.52	0.46	8.84	4.76	30.67	59.90	25.29	1170	1170	1180	1190

Table 2
Experimental conditions.

Case	Coal type	Coal feed rate ($kg·h^{-1}$)	Thermal load (kW)	Load ratio (%)	λ_1	λ_2	λ_p	λ_3	λ_T	MT1 (°C)	HT1 (°C)	SC2 (°C)	Operating condition time (min)	The air distribution ratio at each stage along SC
1	SM	15	112	56.0	0.2	0.35	0.55	0.62	1.17	831	1348	1004	90	9:5:4:8:11:12:11
2	BS	18	107	53.5	0.2	0.35	0.55	0.62	1.17	842	1355	1036	60	
3	YH	16	112	56.0	0.2	0.35	0.55	0.62	1.17	851	1348	1059	55	

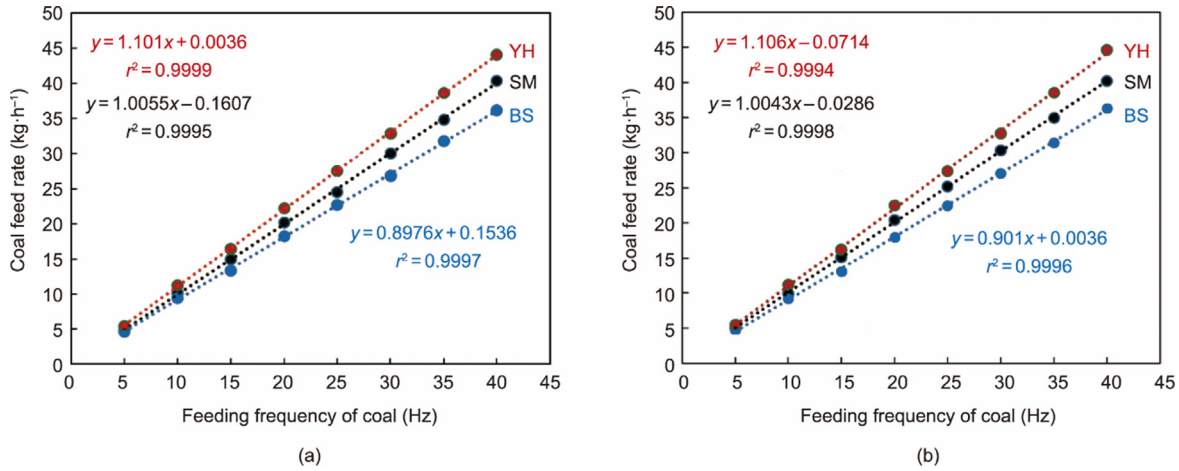

Fig. 3. Calibration curve of feeders: (a) MT1 and (b) MT2.

where $y_{c,MT}$ and $y_{c,HT}$ (kg·kg^{-1}) are the char yields at the outlets of the MT and HT, respectively.

The yields of gas at different reaction stages were calculated based on the nitrogen balance using the following formula:

$$y_{gasMT,i} = \rho_i \times (x_i \times 0.79 q_{airMT})/(x_{N_2} \times m_{coal})(i = CO, H_2, CH_4 ...) \quad (5)$$

$$y_{gasHT,i} = \rho_i \times (x_i \times 0.79 q_{airHT})/(x_{N_2} \times m_{coal})(i = CO, H_2, CH_4 ...) \quad (6)$$

where $y_{gasMT,i}$ and $y_{gasHT,i}$ (kg·kg^{-1}) represent the yield of component i in the gas composition at the MT and HT outlets, respectively; ρ_i (kg·Nm^{-3}) is the density of component i in the gas; q_{airMT} and q_{airHT} (Nm^3·h^{-1}) are the total air flow rates fed into MT and HT, respectively; x_i (%) is the volume fraction of component i, x_{N_2} (%) is the volume fraction of N_2 in the gas, m_{coal} (kg·h^{-1}) is the coal feed rate.

The calculation formulas for combustion efficiency consider the carbon content of the slag, which are shown in Eqs. (11)–(13) of Ref. [23].

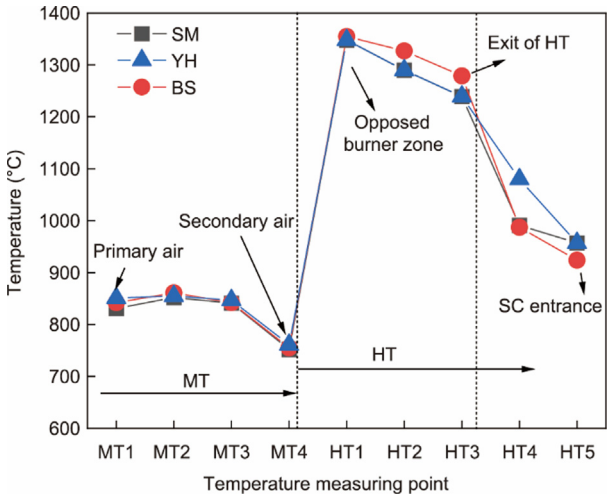

Fig. 4. Temperature distribution of the purification process.

3. Results and discussion

3.1. High temperature purification characteristics of coal

Fig. 4 shows the temperature distribution during the purification process. The operating temperature of the MT is approximately 850 °C, with a temperature difference of less than 30 °C along the path. The circulation of high-concentration carbon particles creates favorable conditions for the release and reduction of volatile nitrogen in coal [24]. The temperature of the gas–solid composite fuel, consisting of coal gas and char produced by the MT, exceeds 700 °C, providing significant sensible heat, which is beneficial for the uniformity and safety of opposed combustion at the bottom of the HT under low-load conditions. The highest temperature in the HT furnace was located in the bottom burner region (HT1), reaching 1350 °C. As the coal gas flows upward, the exit temperature (HT3) decreases to approximately 1200 °C, resulting in a temperature difference of over 150 °C within a furnace height of 1000 mm. This indicates that heat is concentrated and released in the burner region, forming a core high-temperature zone that facilitates the separation of the carbon and inorganic components [25]. On the one hand, the downward 6° inclined opposed burner arrangement in the HT significantly affects the flow, reaction, and heat transfer rates between gases and particles. The high-temperature flame generated by the opposed burners not only provides the necessary heat for the rapid heating of the gas–solid composite fuel from the MT and secondary air but also supplies a large number of free radicals for catalytic oxidation reactions [26]. On the other hand, collisions between gases and particles create intense turbulence and mixing conditions, promoting both homogeneous and heterogeneous reactions. The presence of a core high-temperature zone is a prominent feature of the opposing combustion mode [27]. In this zone, the residual ash particles from the combustion of some particles melt to form liquid slag, achieving the separation of carbon and inorganic components, which is crucial for the stable operation of HT [25,28]. Additionally, no O_2 was detected at the HT outlet, indicating rapid oxygen consumption within the HT, forming a strongly reducing atmosphere that favors the further release and reduction of char nitrogen. In comparison to the presence of MT, directly feeding cold pulverized coal into HT will lead to a decrease in the gasification reaction rate owing to the low solid-phase reaction rate. Consequently, the temperature of the core high-temperature region decreases. These limitations are particularly pronounced for low-grade coals with a low calorific value and low volatile content, often causing incomplete gasification and slagging issues.

Figs. 5(a) and (b) show the main component concentrations of gas at the MT and HT outlets. At the MT outlet, the CO

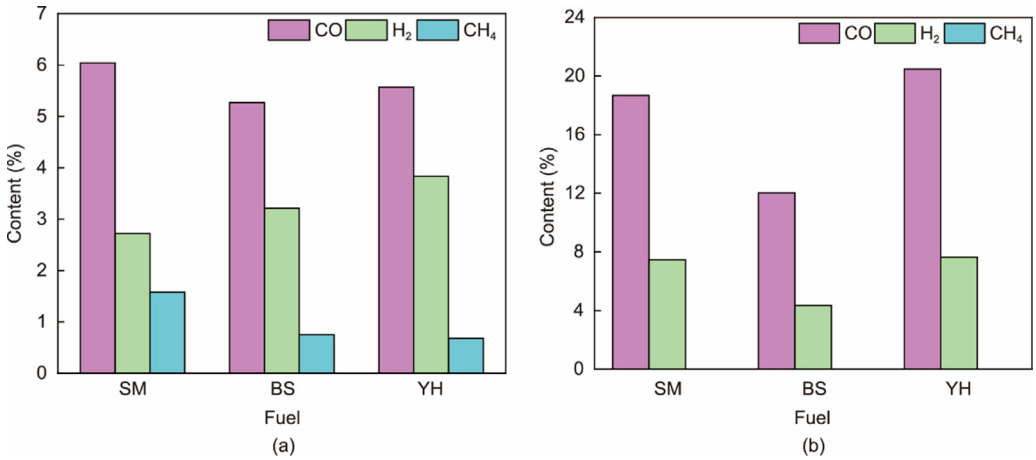

Fig. 5. The contents of CO, H_2, and CH_4 in the purification process (dry basis): (a) MT and (b) HT.

concentration ranged from 5.3% to 6.1%, the H_2 concentration ranged from 2.7% to 3.8%, and the CH_4 concentration remained low, between 0.7% and 1.6%, which is comparable to the results of preheating combustion technology [29]. Through the MT activation process, cold coal particles were converted into high-temperature gas and char composite fuel, facilitating combustion and gasification reactions under low-load conditions. Following an intense high-temperature purification process, the concentrations of CO and H_2 at the HT outlet significantly increase to 18.7%–20.5% and 4.4%–7.6%, respectively. This increase is attributed to the collision of carbon, hydrogen, CO, H_2, and other components in the composite fuel generated within the MT, which rapidly reacts with oxygen under intense turbulence, thereby producing high temperatures. These high temperatures further promoted the conversion of volatile matter and fixed carbon (FC) in coal to CO and H_2, enhancing reactions in Eqs. (7)–(9). This conversion process also facilitates further precipitation of char nitrogen and volatile nitrogen, which are converted to N_2 under a strongly reducing atmosphere. In addition, CH_4 was absent from the HT outlet gas. This absence is due to the strong destruction of C–H bonds at high temperatures, leading to their consumption through reaction (Eq. (11)), and because CH_4, which has a lower ignition temperature than CO and H_2, rapidly reacts with oxygen upon entering the HT. The purification characteristics exhibited by different coal types varied. Among the three types of coal, YH exhibited the highest CO and H_2 concentrations produced through medium-temperature activation and high-temperature purification, followed by SM and BS. This is partly because SM and YH have higher carbon, hydrogen, and volatile matter contents compared to BS coal, and partly because YH coal contains higher levels of alkali metals, which can reduce the activation energy of the gasification reaction and promote Eqs. (7) and (9) [30].

$$2C + O_2 \rightarrow 2CO \quad (7)$$

$$C + CO_2 \rightarrow 2CO \quad (8)$$

$$C + H_2O \rightarrow H_2 + CO \quad (9)$$

$$C + 2H_2 \rightarrow CH_4 \quad (10)$$

$$CH_4 + H_2O \rightarrow CO + 3H_2 \quad (11)$$

Figs. 6(a) and (b) present the conversion rates of C, H, FC, and volatile matter during the purification process of the three types of coal. During the medium-temperature activation reaction, the conversion rates of volatile matter for the three types of coal reached 82.8%–97.7%, FC conversion rates were 39.3%–45.9%, C conversion rates were 34.5%–67.8%, and H conversion rates were 34.8%–65.5%. These findings indicate that the medium-temperature activation reaction significantly promotes the release of volatile matter from coal and its conversion into gaseous products, revealing the dissociation effect on the molecular structure of the fuel. The conversion and consumption of volatile matter are the primary sources of heat for the medium-temperature

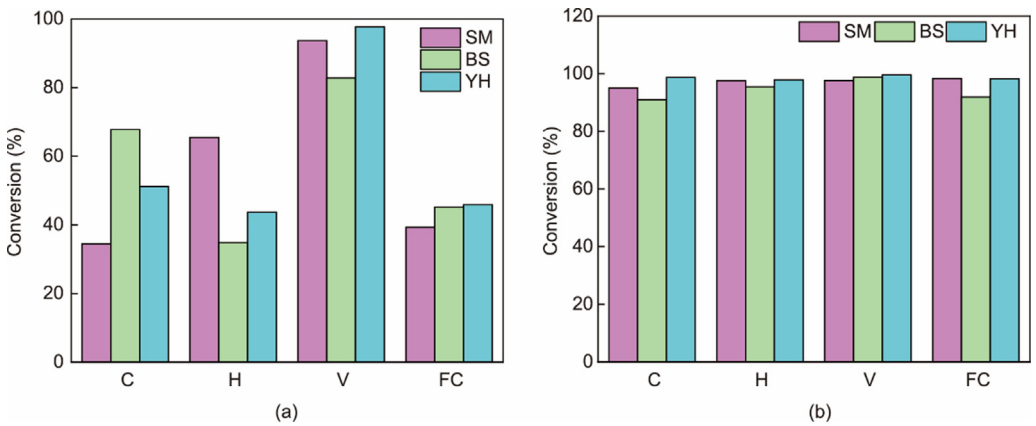

Fig. 6. The conversion rate of components in the purification process: (a) MT and (b) HT. V: volatile matter.

activation processes. After the high-temperature gasification reaction, the conversion rates of volatile matter for the three types of coal increased to 97.6%–99.6%, indicating that almost all remaining volatile matter was converted during the high-temperature purification process. The conversion rates of FC increased to 91.9%–98.3%, with a greater increase than that of volatile matter, suggesting that temperature is a decisive factor in FC conversion. The FC is the primary heat source for the high-temperature gasification reaction. Additionally, the conversion rates of C and H significantly increased to over 91%, further demonstrating that the intense mixing and turbulence in the gas–solid composite fuel opposed combustion mode greatly promoted the release of C and H, resulting in higher concentrations of CO and H_2. Volatile nitrogen, as part of the volatile matter, is the main source of NO_x precursors HCN and NH_3, whereas char nitrogen primarily exists in FC. The different conversion characteristics of volatile matter and FC in the MT and HT processes imply that the conversion characteristics of volatile nitrogen and char nitrogen also differ between these two processes.

To verify the impact of high-temperature gasification reactions on the activity of solid-phase char, Brunauer–Emmett–Teller (BET) analysis was conducted on three types of coal and their respective chars during the purification process, as shown in Figs. 7(a)–(c). Compared with raw coal, the specific surface area and pore volume of char at the MT outlet increased by 5–140 times and 2–15 times, respectively, with a significant increase in the number of micropores. This indicates that the medium-temperature activation process at approximately 850 °C significantly developed the pore structures of carbon particles. This development was due to the substantial release of volatile matter from the pores during the medium-temperature activation reaction, causing the coal particles to soften, expand, and form a porous structure, thereby increasing the number of micropores [31]. The larger specific surface area and pore volume provided more reaction sites, which helped increase the oxygen content within the char particles and enhance the diffusion and flow rates of gaseous products, thereby improving the reaction rate. The active char at the MT outlet strengthened the opposed combustion under a low load and formed a core high-temperature zone. Furthermore, owing to the high-speed jet collision of the gas–solid composite fuel during the high-temperature purification process, the gas–solid reaction is further enhanced, and the pore structure of the carbon particles is further developed. The specific surface area and pore volume of the char at the HT outlet increased by 10–150 times and 7–40 times, respectively, compared to raw coal, with a further increase in the number of micropores. The high-activity char at the HT outlet was conducive to the efficient combustion of carbon particles in the SC under a low load. Additionally, in the catalytic NO_x reaction of char, the active sites and free radicals on the char surface can adsorb NO molecules and generate N_2 and CO (Eq. (12)), thereby promoting the reduction and conversion of volatile nitrogen in MT and char nitrogen in HT to N_2. Among the three types of coal, the char activity of YH was significantly higher than those of SM and BS, with the most notable activation effect, achieving a specific surface area of over 500 $m^2 \cdot g^{-1}$. This further explains the highly purified characteristics of YH, as shown in Fig. 6.

$$NO + C \rightarrow N_2 + CO \quad (12)$$

Fig. 8 presents the microscopic morphology analysis of the three types of coal and char. The surfaces of the three raw coals were dense and highly graphitized. However, after medium-temperature activation and high-temperature gasification reactions, the pore structures on the particle surfaces developed significantly. Under intense particle collisions and gas–solid flow, reactants combine with carbon to form carbonyl and carboxyl groups, breaking the carbon bonds in the aromatic structure of the coal and resulting in the formation of more micropores. This substantially increased the specific surface area and reactivity [16].

To further compare and analyze the carbon framework stability and reactivity of raw coal and char, the Raman fitting results of the char were subjected to integral quantitative analysis, as shown in Figs. 9(a)–(c). I_G represents the integrated intensity of the G band in the Raman spectrum, I_{D1} refers to the integrated intensity of the D1 band, I_{D3+D4} corresponds to the sum of the integrated intensities of the D3 and D4 bands, and I_{ALL} denotes the total integrated intensity of all characteristic bands in the entire Raman spectrum. The ratio I_{D1}/I_G is employed to evaluate defect density or structural disorder, I_{D3+D4}/I_G is used to assess the content of amorphous carbon and the influence of impurities, and I_G/I_{ALL} serves as an indicator of the degree of graphitization. After medium-temperature activation and high-temperature gasification reactions, the I_G/I_{ALL} ratios of the three types of coal decreased, indicating a reduction in the proportion of stable graphite structures in the char. This is primarily due to the depolymerization and devolatilization of coal particles during the purification process, which causes the carbon chains in the aromatic layer structure to break and form small molecular volatiles. The breaking of large molecular carbon chains helps reduce the degree of graphitization of the carbon framework [32]. The breaking of large molecular carbon chains also promoted the transformation of stable graphite structures into disordered active defect structures, as evidenced by the increase in the I_{D3+D4}/I_G ratio. The increase in the number of small aromatic ring structures also enhances the number of active sites on the particle surfaces, as indicated by the increase in the I_{D1}/I_G ratio. The fewer the ordered structures in the char, the higher its reactivity [33]. Therefore, medium-temperature activation and high-temperature purification processes effectively enhance the reactivity of char,

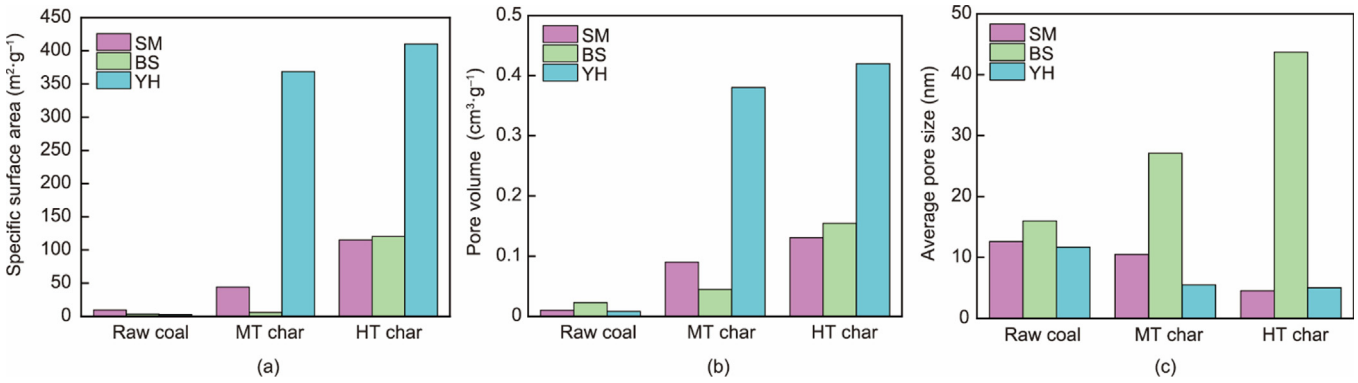

Fig. 7. Analysis of (a) specific surface area, (b) pore volume, and (c) average pore size of raw coal and char.

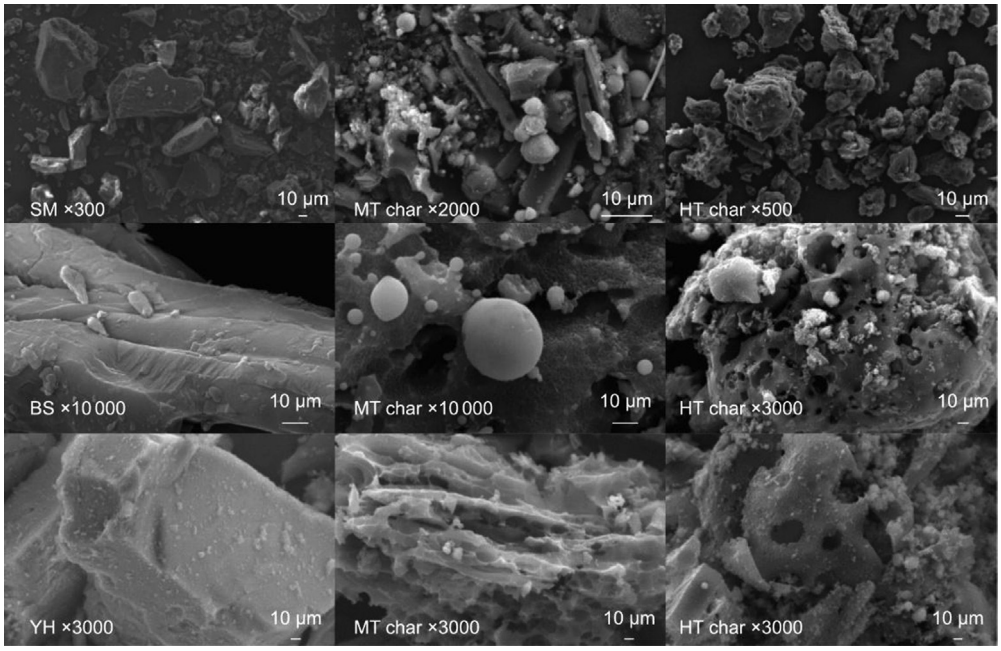

Fig. 8. Microscopic morphology analysis of raw coal and char.

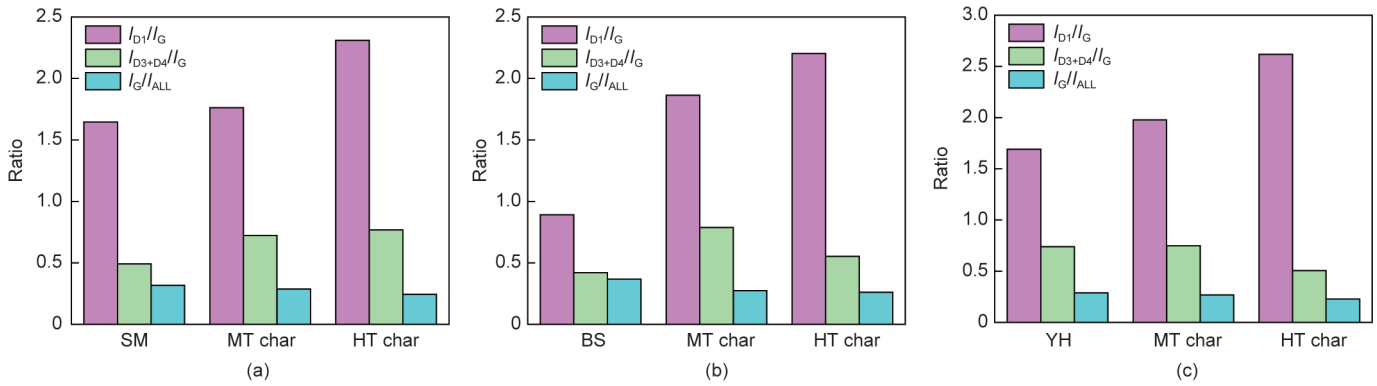

Fig. 9. Raman analysis of raw coal and char: (a) SM, (b) BS, and (c) YH.

thereby improving the combustion stability of the fuel under low-load conditions.

One of the key roles of MT lies in its ability to activate and modify coal particles under fluidized conditions, which significantly enhances the reaction rate and efficiency of high-temperature gasification within the HT. This effect is particularly critical for the formation of a core high-temperature zone near the HT burner plane. In addition, MT effectively mitigated the reactivity differences among various coal types. It demonstrates excellent modification performance, even for low-grade fuels with low calorific value and low volatile content [25]. By activating and modifying the coal feed, MT shortens the required reaction time within the HT, allowing for a more compact HT design (Fig. 2). This contributes to a reduction in the overall system cost and addresses the challenge of the low gasification efficiency commonly observed in atmospheric gasifiers.

Efficient separation of inorganic components during coal purification is crucial for achieving high-value utilization and reduction of these components. Fig. 10 illustrates the removal of inorganic components during high-temperature purification. In coal, inorganic components are primarily dispersed within, and bound to, organic matter. In the high-temperature region generated by the opposed combustion of the gas–solid composite fuel, as the carbon conversion rate increases, the carbon particles gradually shrink. When the purification temperature exceeded the coal ash melting temperature, the coal char particles continued to react in the shrinking particle mode, leading to ash melting. The molten ash flows towards the particle edges, moving from the surface of one carbon particle to the surface of other carbon particles, and fuses to form liquid slag. This process completes the mineral-phase reconstruction of the inorganic components. Uncaptured inorganic components remain in the unreacted char [25]. After melting and rapid cooling, the inorganic components form a slag, which appears bright black.

Fig. 11 shows the mineral composition of the slag. The presence of humps detected at 20°–38° in the slags of the three types of coal indicates the existence of an amorphous glass phase. During the cooling process, solid crystals precipitated from slag. The slag primarily consists of a tetrahedral network formed by Si–O bonds. The higher the content of acidic oxide SiO_2, the lower the content of precipitated quartz crystals, indicating a higher degree of network polymerization in the slag [34,35]. A high SiO_2 content facilitates

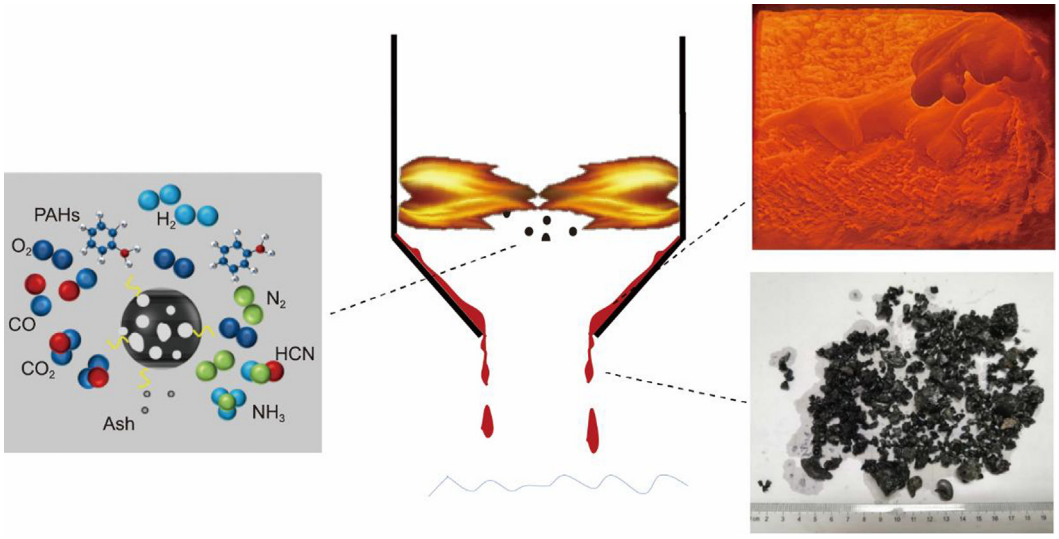

Fig. 10. Schematic diagram of inorganic component removal in purification process. PAHs: polycyclic aromatic hydrocarbons.

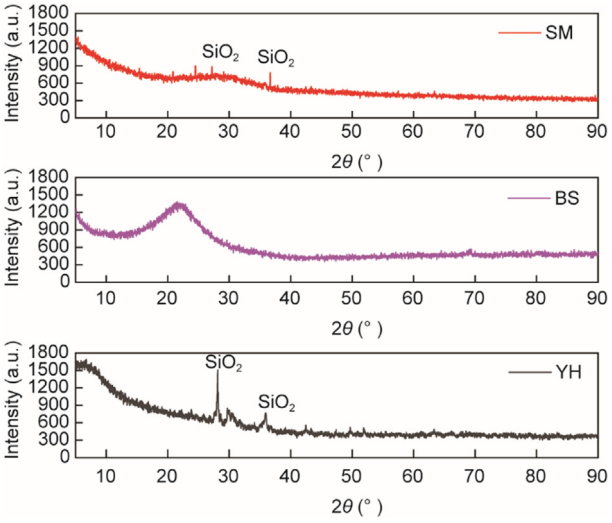

Fig. 11. Analysis of slag mineral composition.

the flow and discharge of high-temperature slags. The slag removed by the purification system can be further utilized for the production of microcrystalline glass or fiber drawing [36].

Fig. 12 shows the microscopic morphology of the slag. The slag primarily appeared as dense, smooth blocks, but some uneven wrinkles and a small amount of flocculent material attached to the surface of some particles were also observed. The surface element analysis results in Fig. 13 show that the slag is mainly composed of Ca, Si, and Al, but the surface of the slag also contains a certain amount of carbon with a content of less than 2.5%. This may be due to the entrainment of carbon particles during slag flow. Some studies suggest that during the formation of liquid slag, highly reactive carbon in the coal participates in the reaction, whereas a small amount of less reactive carbon is encapsulated by the molten slag [25].

Fig. 14 shows the carbon conversion and ash removal rates during the high-temperature purification process for different fuels. A positive correlation was observed between the carbon conversion and ash removal rates during the high-temperature purification process. A higher carbon conversion rate indicates that more organic matter in the particles is converted, and more inorganic components are separated from the organic matter and converted into liquid slag under high-temperature and strongly reducing conditions. The removal rate of inorganic components during the high-temperature purification process reaches 62%–85%, indicating that the carbon-ash separation process is essentially achieved in the purification system [19]. Under low-load conditions, combustion/gasification tends to be unstable, making it difficult to sustain a robust core high-temperature zone. The MT stage generates a high temperature gas–solid composite fuel (> 700 °C) under fluidized conditions, significantly enhancing fuel reactivity and gas–solid uniformity. This mitigates the adverse effects of load reduction and enables rapid, efficient, and stable gasification/combustion within the HT stage, even at low loads, thereby establishing a stable core high-temperature zone and achieving efficient carbon conversion and effective inorganic component separation.

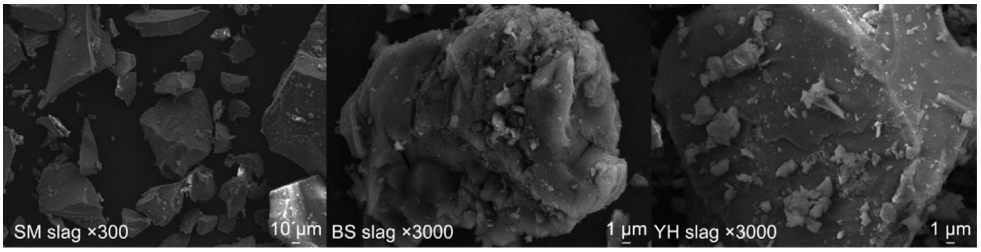

Fig. 12. Analysis of slag microstructure.

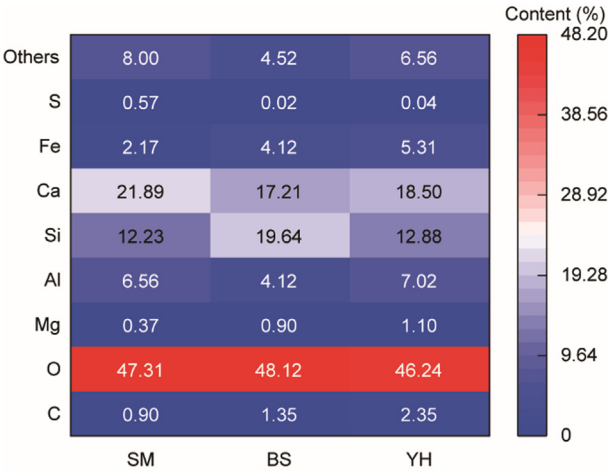

Fig. 13. Surface element analysis of slag.

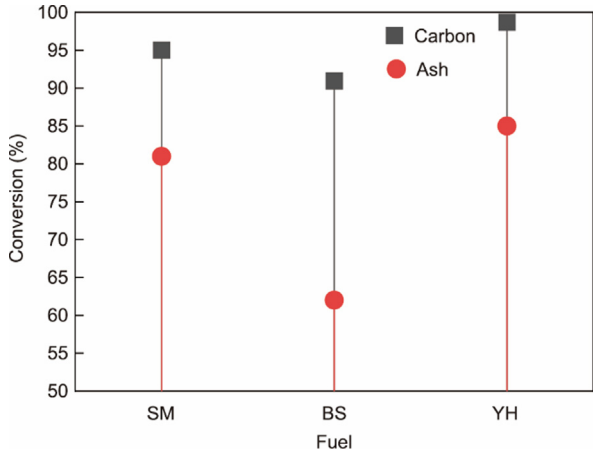

Fig. 14. Carbon conversion rate and ash removal rate in purification process.

3.2. Precipitation and transformation of coal N during purification process

HCN and NH_3 are the two main nitrogen-containing pollutants in a reducing atmosphere that may be converted to NO_x during subsequent combustion processes. Fig. 15 shows the variation in NH_3 and HCN concentrations generated during the purification process for the three types of coal. During the medium-temperature activation process, the NH_3 concentration in the coal gas is relatively high, reaching 150–250 ppm, whereas the HCN concentration is 35–46 ppm, which is significantly lower than that of NH_3. After the high-temperature purification process, the NH_3 concentration in the coal gas significantly decreases to 25–50 ppm, and HCN was absent. This indicates that NH_3 and HCN were primarily generated during the medium-temperature activation reaction of coal and were converted during the high-temperature gasification reaction. The nitrogen in coal exists mainly in the form of aromatic nitrogen. The medium-temperature activation process is primarily volatilization, during which most of the volatile nitrogen is released. Heterocyclic nitrogen decomposes into –CN and –N, which combine with free radicals such as –H, –C, and –O to form NO, HCN, and NH_3, while NO is rapidly reduced in a strongly reducing atmosphere [37]. According to the coal nitrogen conversion model proposed by Smoot and Smith [38] and Haynes [39], HCN is mainly generated during the early pyrolysis stage of coal, and large amounts of OH and H free radicals generated during the volatilization stage can convert HCN to NH_3. Therefore, the NH_3 concentration in the coal gas at the MT outlet was higher than that in HCN·NH_3 can be converted to N_2 in a reducing atmosphere [40], and the intense reactions near the HT burner generate more OH and H free radicals that can convert HCN to NH_3. Part of the NH_3 entering the HT is reduced to N_2 (Eqs. (13) and (14)), resulting in a lower NH_3 concentration at the HT outlet [17]. HCN is extremely unstable at high temperatures and is generally considered to be oxidized to N_2 in a reducing atmosphere and to NO in an oxidizing atmosphere, following reaction pathways (Eqs. (15) and (16)). Because no NO_x was present in the coal gas at the HT outlet, it can be inferred that part of the NH_3 and all of the HCN were converted to N_2 during the high-temperature purification process. The highly active char surface at the MT outlet also provided numerous active sites for the conversion of char nitrogen to N_2 during the char nitrogen release process.

$$NH_3 + OH/O/H \rightarrow NH_2 + H_2O/OH/H_2 \quad (13)$$

$$NH_2 + NO \rightarrow N_2 + H_2O \quad (14)$$

$$HCN + 5/4O_2 \rightarrow 1/2N_2 + CO_2 + 1/2H_2O \quad (15)$$

$$HCN + 7/4O_2 \rightarrow NO + CO_2 + 1/2H_2O \quad (16)$$

Fig. 16 presents the proportions of different nitrogen forms in the three types of coal during the purification process. In the MT, volatile nitrogen is primarily converted to N_2, with a conversion

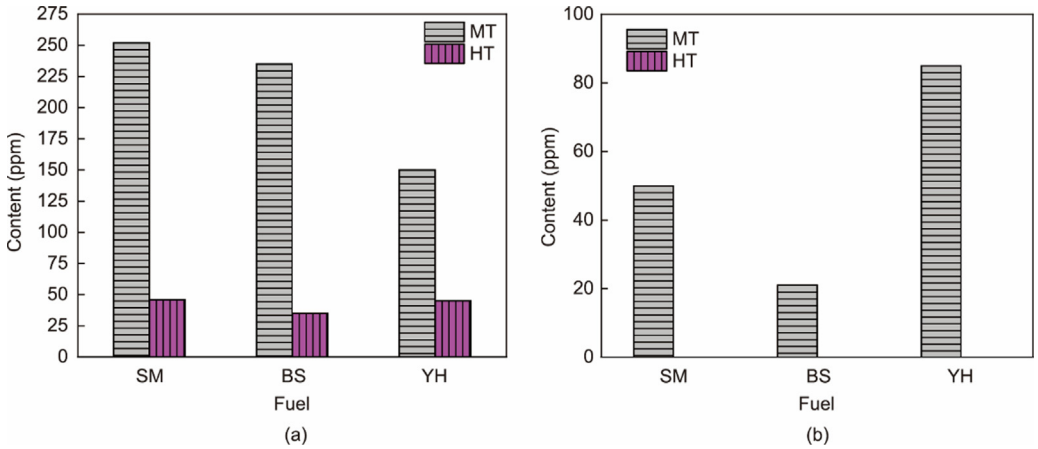

Fig. 15. The changes of (a) NH_3 and (b) HCN content in the purification process.

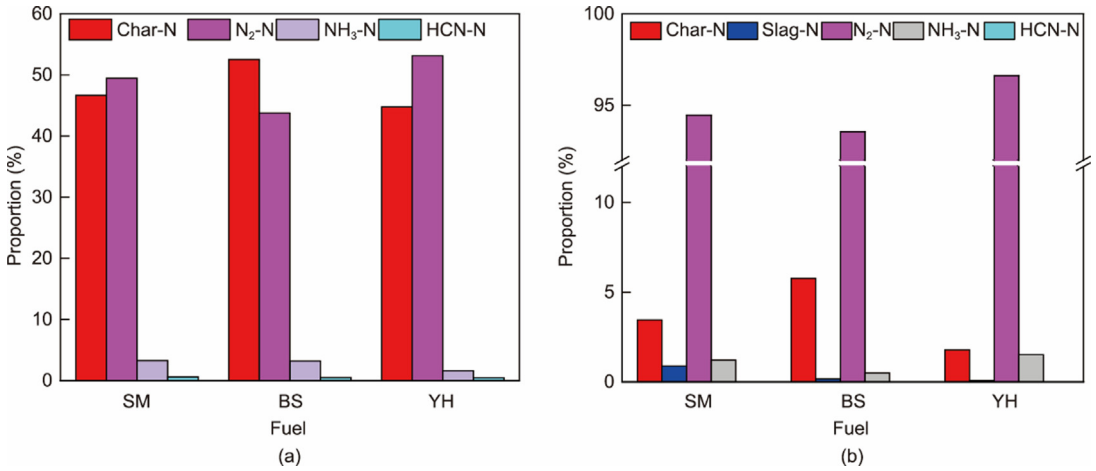

Fig. 16. Different forms of N content in the purification process: (a) MT and (b) HT.

rate of 43.8%–53.1%, the proportion converted to NH_3 is 1.6%–3.3%, and the proportion converted to HCN is only 0.5%–0.6%. Additionally, 44.8%–52.5% of the coal nitrogen remains in the char as char nitrogen. YH and SM, which have higher volatile contents, also exhibit higher conversion rates of coal nitrogen to N_2. The medium-temperature activation process mainly involved the release of volatile nitrogen and its reduction to N_2. Char with a developed pore structure plays a dominant role in the heterogeneous reduction of NO, and the presence of CO significantly improves the kinetics of NO reduction. Furthermore, during the high-temperature purification process, the conversion rate of coal nitrogen to N_2 reaches 93.6%–96.6%, an increase of 43.5%–49.8% compared to the medium-temperature activation process, while the proportion of char nitrogen decreased to 1.8%–5.6%. This indicates that the high-temperature purification process primarily involves the release and conversion of char nitrogen to N_2, accompanied by substantial consumption of FC. The released char nitrogen combines with free radicals such as –H, –C, and –O to form NO, HCN, and NH_3, which are then converted to N_2 (Eqs. (13)–(15)). Additionally, a small portion of the slag nitrogen present in the inorganic components is discharged with the slag, with a very low content that does not participate in the combustion reaction process. The 1.8%–5.6% of char nitrogen is the main source of NO_x conversion during the subsequent combustion processes. Therefore, MT enhances the conversion of fuel nitrogen to N_2 by leveraging a fluidized high-carbon circulation process that strengthens the mixing and contact time between the char and coal gas. This mechanism effectively promoted the reduction of highly reactive volatile nitrogen species by char, achieving near-complete conversion of volatile nitrogen into N_2, NH_3, and HCN. As a result, the nitrogen conversion occurring within HT primarily involves the reduction of char-bound nitrogen.

To further characterize the transformation mechanisms of solid-phase nitrogen during the high-temperature purification process, X-ray photoelectron spectroscopy (XPS) analysis was conducted on the nitrogen-containing functional groups in the raw coal and char. The analysis focused on four nitrogen species: pyridinic nitrogen (N-6), pyrrolic nitrogen (N-5), quaternary nitrogen (N-Q), and nitrogen oxide (N-X). The relative contents of these nitrogen species in the coal and char were quantified through integration, thereby elucidating the changes in nitrogen forms during the purification process, as shown in Fig. 17. Among the three types of coal, N-5 predominates, with a relative content of 39.4%–62.5%, indicating that the nitrogen in coal predominantly exists in the form of five-membered ring pyrrolic nitrogen. After the medium-temperature activation process, nitrogen-containing functional

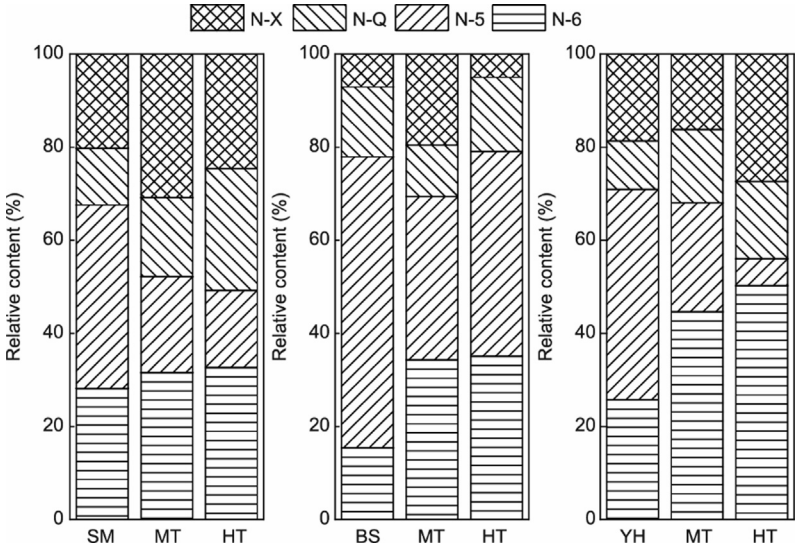

Fig. 17. Relative content of nitrogen-containing functional groups.

groups undergo cleavage, and nitrogen is primarily released from the coal in the form of NH_3 and HCN [41]. The relative content of N-5 decreases to 20.6%–35.1%, while the relative contents of N-6, N-Q, and N-X increased. At high temperatures, N-5 was relatively reactive and partially converted to N-6 and N-X, and the more stable N-Q. Nitrogen that migrates to the edges of the carbon rings exists more in the form of N-6, further increasing the content of N-6. Following the high-temperature purification process, the relative content of N-5 in the char further decreases to 5.8%–43.9%. The higher temperatures caused the reactive N-5 to convert more to N-6 and N-Q, with the remaining N-5 existing more in the form of pyridone within the char particles. Nitrogen in coal is ultimately released in the form of NH_3, HCN, and N_2, with N-Q primarily converting to NH_3, while portions of N-5 and N-6 generate HCN [42].

Based on the ash balance calculations, the mass distributions of combustible materials in coal gas, slag, and char after medium-temperature activation and high-temperature gasification reactions for 1 kg of coal are shown in Fig. 18. After the medium-temperature activation process, the mass of solid-phase combustibles was approximately 0.16–0.56 kg, and the mass of gas-phase combustibles was approximately 0.21–0.33 kg. This indicates that the medium-temperature activation process was primarily dominated by heterogeneous reactions, with char playing a crucial role in the reduction of nitrogen. Following the high-temperature purification process, owing to the significant increase in the carbon conversion rate and the separation of inorganic components, the mass of solid-phase combustibles is only 0.001–0.040 kg, which is much lower than the mass of gas-phase combustibles (0.77–1.25 kg). The purified char possesses high physical sensible heat (> 900 °C), and the homogeneous combustion reaction rate of high-temperature purified coal gas (> 900 °C) is also high, with high physical sensible heat. This implies that, compared with the traditional heterogeneous combustion reactions of coal, the combustion of coal after high-temperature purification shifts to homogeneous gas-phase combustion reactions. The FC conversion rate of over 92% during the purification process, as shown in Fig. 6, also supports this. Gas-phase fuel is more conducive for achieving MILD combustion [43], which benefits the combustion process and pollutant emission control under low-load conditions.

Fig. 19 presents a schematic of the coal purification process. The core of the medium-temperature activation mechanism is the conversion of coal particles into coal gas and highly active char, which facilitates the gasification reactions under low-load conditions, achieving a conversion of 43.8%–53.1% of coal nitrogen to N_2. The high-temperature purification mechanism, through intense gasification reactions, separates 62%–85% of inorganic components, effectively achieving the separation of carbon and inorganic components. The coal particles are converted into a gas-phase fuel primarily composed of CO and H_2, and the pore structure of the char is further developed, which is conducive to stable combustion under low-load conditions. During this process, 96.6% of the coal nitrogen was reduced to N_2. Although the inclusion of MT adds a certain degree of complexity to the system, it offers significant advantages in coal particle activation and modification, enhancement of reaction intensity, promotion of fuel nitrogen reduction, and improvement of operational stability under low-load conditions. The authors' research team is currently optimizing the burner design and developing a modular integration of MT and HT units, which is expected to further simplify the system architecture and reduce equipment investment in the future.

3.3. Combustion characteristics of gaseous fuel

The high-temperature gas–solid composite fuel generated by the HT enters the SC combustion chamber in a swirling motion at a speed of approximately 10 $m{\cdot}s^{-1}$. The required tertiary air is introduced through the A1–A7 nozzles along the path, where it reacts with the fuel. The structure of each nozzle is shown in Fig. 2, and the air distribution ER and flow rates of each nozzle are shown in Fig. 20. The boundary is defined at an overall ER of 1 along the SC path, with regions having an overall ER less than 1 defined as the reduction zone, and regions with an overall ER greater than 1, defined as the oxidation zone. The A1–A5 nozzles are located in the reduction zone, with each stage using an eight-nozzle opposed structure, while the A6 and A7 nozzles are located in the oxidation zone, using an eight-nozzle non-opposed structure. Under the experimental conditions, the air distribution ER in the reduction zone was 0.37, with a length of 3500 mm, and in the oxidation zone, it was 0.23, with a length of 1500 mm. The flow rate of A2 nozzle was 20 $m{\cdot}s^{-1}$, whereas the flow rates of the other nozzles exceeded 50 $m{\cdot}s^{-1}$. The high-speed radial flow of the oxidant created a strong internal disturbance and mixed with the axially flowing composite fuel. Unlike conventional cold coal powder, which directly enters the furnace for combustion, the high-temperature gas–solid composite fuel can combust within milliseconds at temperatures above its ignition point.

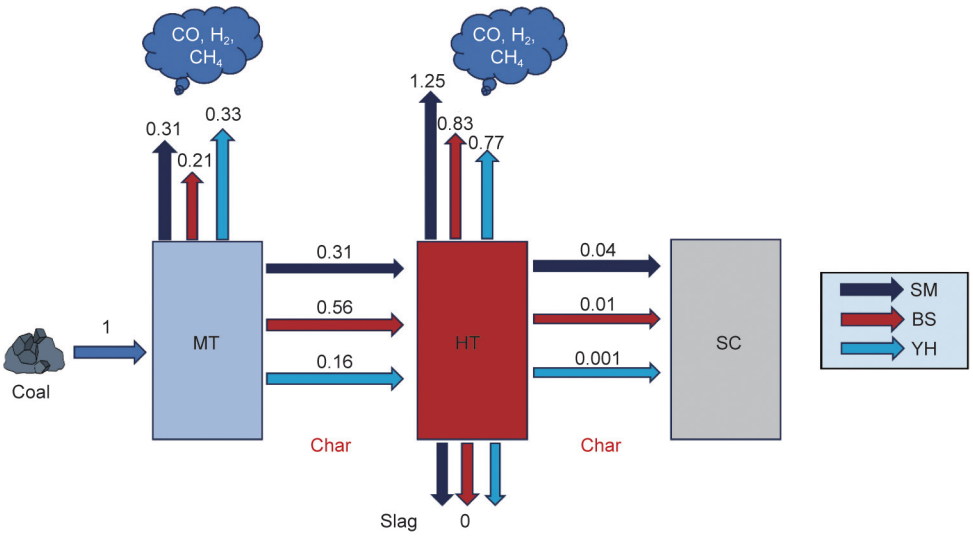

Fig. 18. Mass distribution of gas phase combustible components and solid phase combustible components in unit mass fuel purification process ($kg{\cdot}kg^{-1}$).

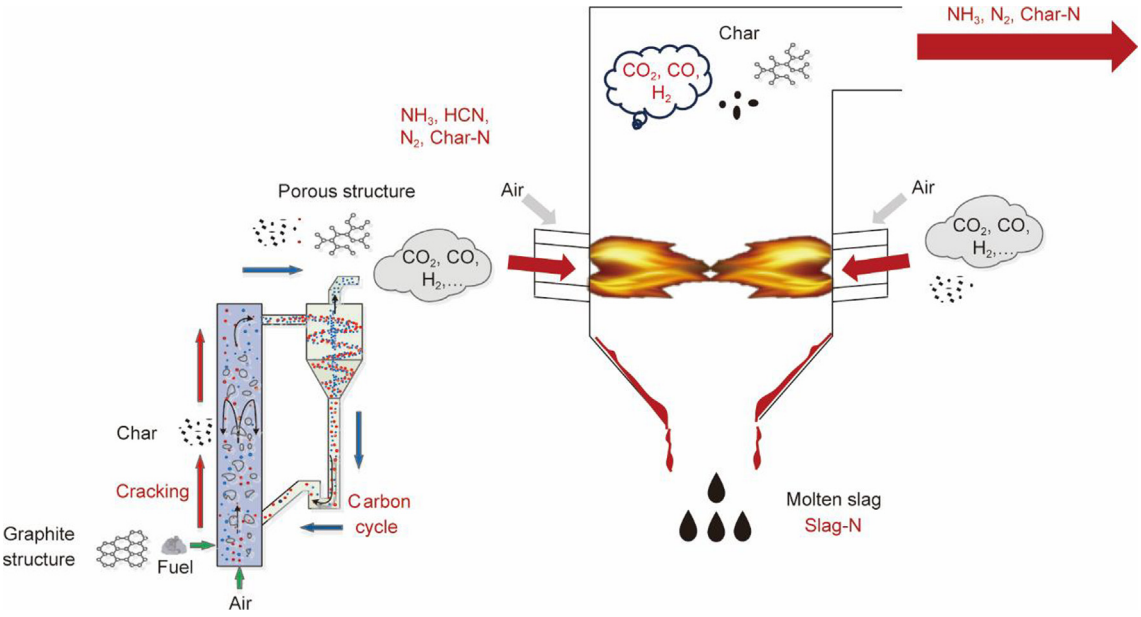

Fig. 19. High temperature purification process diagram.

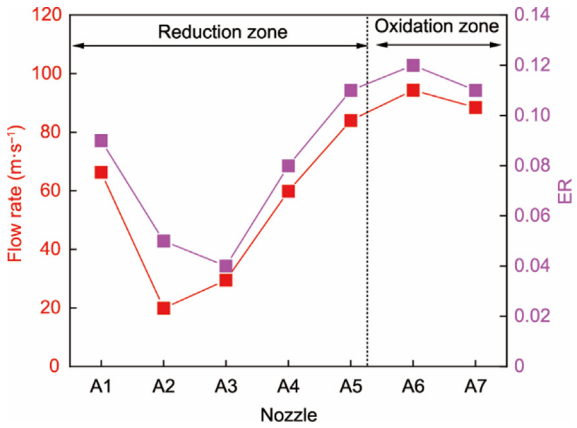

Fig. 20. ER and flow velocity of air along the nozzle of SC.

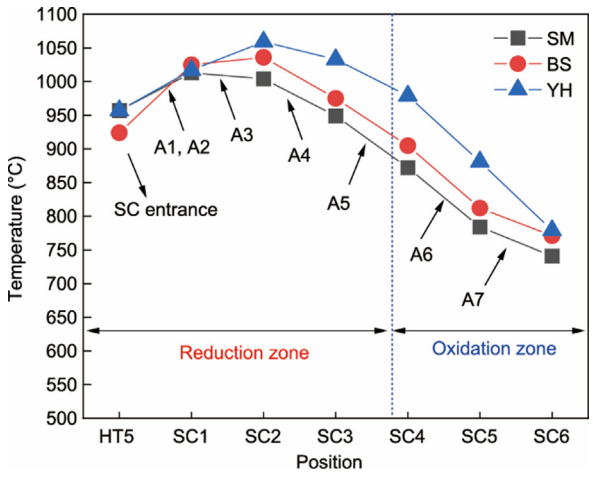

Fig. 21. Temperature along the SC.

Fig. 21 shows the axial temperature distribution in the SC, and Fig. 22 presents the changes in the CO and H_2 concentrations along the SC axis. After the introduction of staged air through the A1–A3 nozzles, the temperature in the SC rapidly increased, reaching a maximum of 1013–1060 °C, with no thermal NO_x produced. This is because the gas-phase fuel, primarily composed of CO and H_2, enters the SC in a swirling motion and rapidly reacts homogeneously with oxygen under a strong lateral disturbance and mixing of the oxidant, releasing heat. The disturbance was most intense, and the mixing was most uniform in the composite fuel nozzle region, resulting in the highest temperatures. The rapid decrease in the CO and H_2 concentrations at the SC inlet also indicates this. Within the 3500 mm reduction zone, the temperature difference between SC1–SC4 points is within 100 °C, indicating relatively uniform temperatures. This suggests that the deep air distribution in the reduction zone suppresses the combustion rate of the gas-phase fuel, allowing for a slow heat release and MILD combustion. The slow release of residual char nitrogen and increased reduction time favor the conversion to N_2 [21]. The concentrations of CO and H_2 gradually decreased as the oxidant was gradually introduced, with CO concentrations at the reduction zone exit ranging from 2.5%–5.8% and H_2 concentrations from 0.1%–1.8%. The oxidation zone primarily involves the burnout of residual CO, H_2, and char, with temperatures dropping below 950 °C. The burnout of char in the oxidation zone signifies the complete release of char nitrogen, and controlling the temperature in the oxidation zone helps regulate the combustion intensity of char, inhibiting the conversion of char nitrogen to NO_x [44].

MILD combustion is characterized by a volumetric low-reaction-rate combustion zone and typical medium-to-low-temperature combustion characteristics, which are associated with high-speed jets and intense turbulent mixing. This is typically achieved using high-speed jets or preheated fuels [45]. Figs. 23(a) and (b) illustrate the schematic diagrams of traditional coal powder high-speed jet combustion and high-temperature gas–solid composite fuel high-speed jet combustion using this technology, respectively. Traditional coal powder jet combustion involves particle preheating, moisture evaporation, devolatilization, and burnout. In this experiment, the SC primarily involved the combustion of high-temperature gas-phase CO and H_2, with an inlet temperature exceeding 950 °C, a flow rate of 10 $m \cdot s^{-1}$, and an oxidant nozzle flow rate exceeding 50 $m \cdot s^{-1}$. There is no particle preheating,

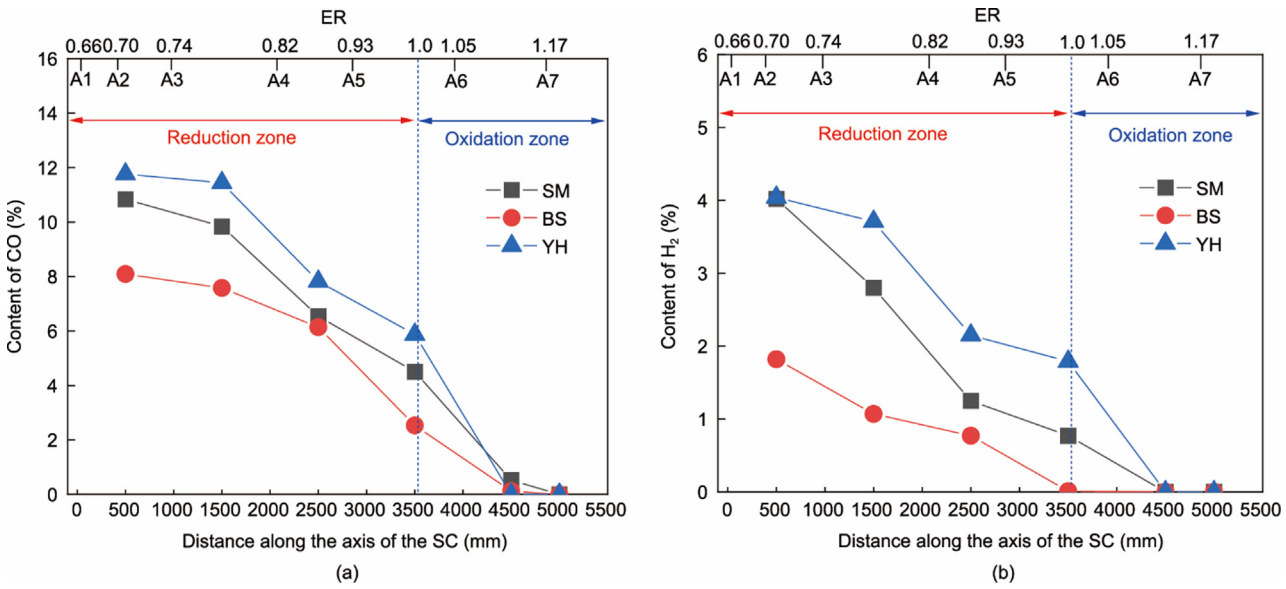

Fig. 22. Changes of (a) CO and (b) H_2 content along the SC.

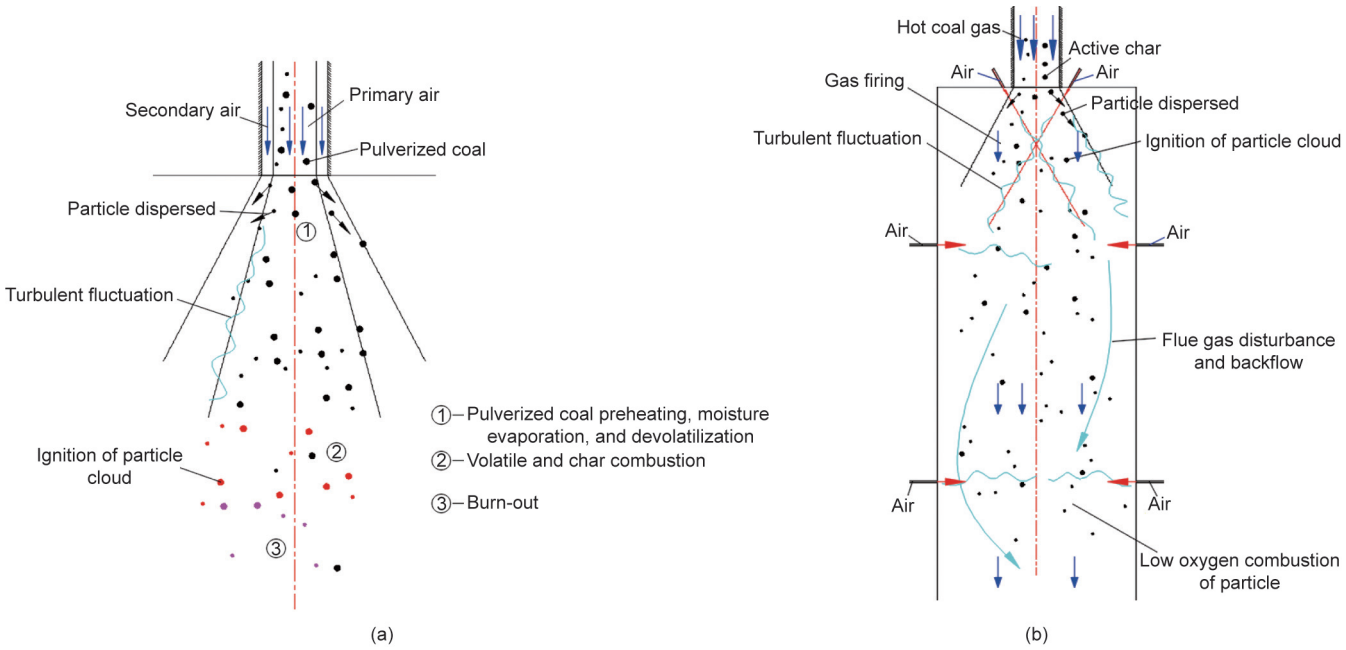

Fig. 23. (a) Traditional pulverized coal jet combustion and (b) high temperature gas–solid composite fuel jet combustion process schematic.

moisture evaporation, or devolatilization process, creating favorable conditions for achieving MILD combustion. Cavaliere and De Joannon [46] suggested that MILD combustion occurs when the reactant inlet temperature exceeds its ignition temperature, and the maximum temperature difference between the combustion temperature and inlet temperature is lower than the ignition temperature of the reactants. In SC, staged oxidant injection allows combustion reactions to occur over a larger spatial scale rather than being confined to the flame front region. This reduces the axial peak combustion temperature, and the fuel remains in a low-oxygen and low-temperature-gradient environment. Limited-rate chemical reactions along the path play a crucial role in the MILD combustion process, and the combustion of coal gas and char is different from that of traditional coal powder flames. Additionally, the high-speed swirling motion of the fuel nozzles and radial nozzle arrangement significantly enhanced the disturbance and mixing in the SC reduction zone, further reducing the peak temperature. Kumar et al. [47] defined MILD combustion as a combustion mode with a spatially averaged temperature fluctuation below 15%. In this experiment, the temperature fluctuations in the SC reduction zone for the three types of coal were only 2.9%, 4.5%, and 3.7%, with overall temperature fluctuations of 14.4%, 13.4%, and 12.5%, respectively. Therefore, it can be considered that the combustion of gas-phase fuel in the SC is a MILD combustion process, which is beneficial for improving combustion efficiency and controlling NO_x formation under low-load conditions.

3.4. Migration and transformation of N in combustion process

Fig. 24 illustrates the variation in the concentrations of the nitrogen-containing gas-phase components NH_3, HCN, and NO along the SC·NH_3, a precursor of NO_x in the gas entering the SC,

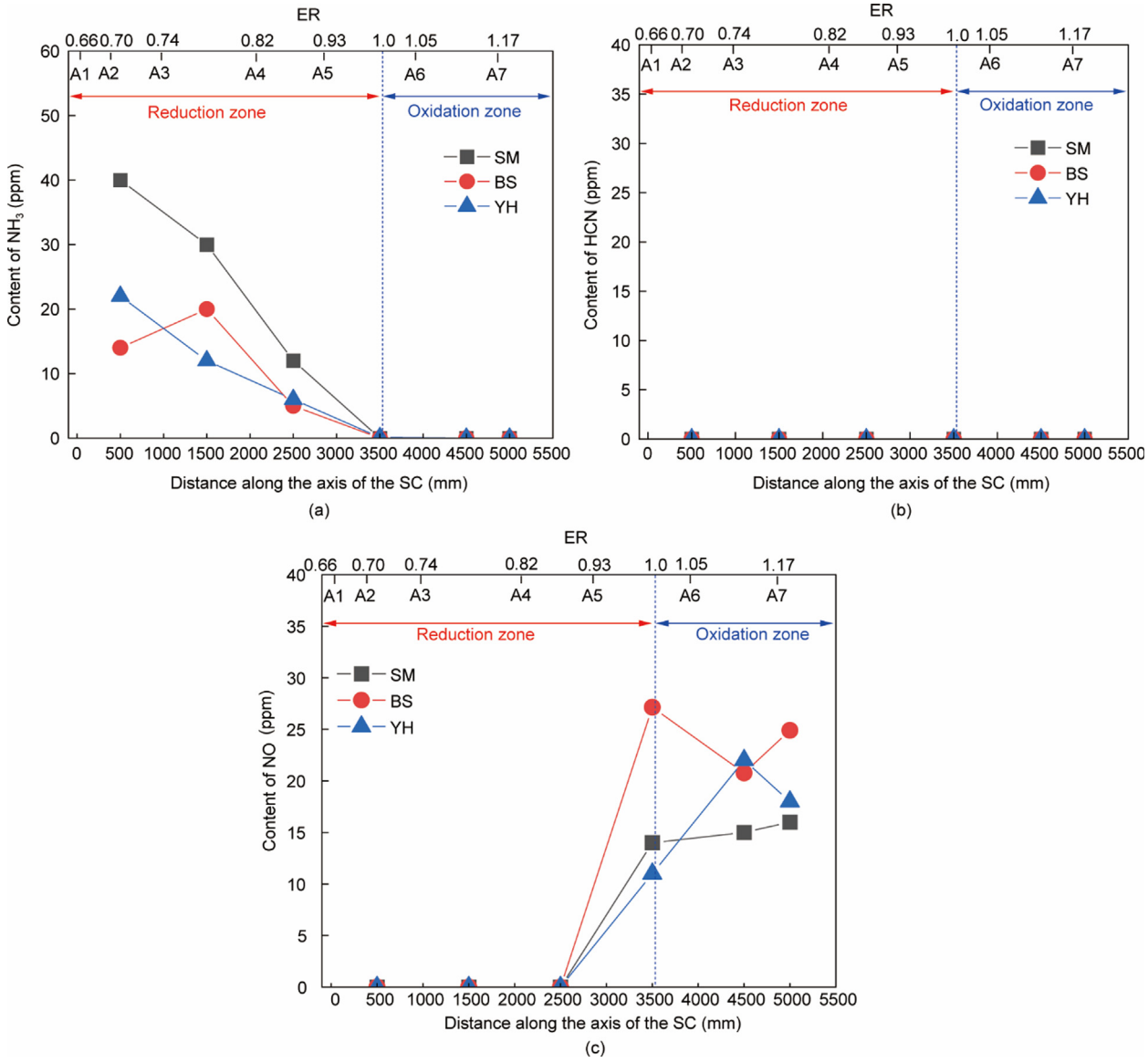

Fig. 24. The content change of nitrogen-containing components along SC: (a) NH_3, (b) HCN, and (c) NO.

had a concentration of 25–50 ppm (Fig. 14). Following the staged air injection in the SC reduction zone A1–A5, the NH_3 concentration gradually decreased, reaching 0 ppm at the outlet of the reduction zone (ER approximately 1). Generally, NH_3 is converted to NO in an oxidizing environment and to N_2 in a reducing environment. Before the staged air injection at A5, the SC was in a reducing atmosphere and NO was not detected, suggesting that NH_3 was more likely converted to N_2 in the reduction zone via pathways (Eqs. (13) and (14)). After staged air injection at A5 (ER = 0.93), NO begins to form in the oxidation zone, and some unconverted NH_3 may be oxidized to NO (Eqs. (17)–(19)).

$$NH_3 + OH/O/H \rightarrow NH_2 + H_2O/OH/H_2 \quad (17)$$

$$NH_2 + O \rightarrow HNO + H \quad (18)$$

$$HNO + OH \rightarrow NO + H_2O \quad (19)$$

The HCN concentration at the SC inlet was 0 ppm (Fig. 14) and no new HCN was generated throughout the combustion process. This is because volatile matter, the primary source of HCN, was almost entirely converted during the high-temperature purification process, rendering HCN unstable at high temperatures. Before the staged air injection at A5 (ER < 0.93), NO formation was not detected in the SC, primarily because of the presence of abundant free radicals on the surface of the char in the reduction zone, which could reduce NO. Additionally, a high concentration of CO significantly improved the kinetics of NO reduction, leading to the reduction of NO formed from NH_3 and char N to N_2. Homogeneous reactions (Eqs. (20) and (21)) and heterogeneous reactions (Eq. (21)) are the two main pathways for NO reduction. As CO, H_2, and residual char were consumed in the oxidation zone, NO was predominantly formed in the SC oxidation zone. After the staged air injection at A5, the NO concentration rapidly reached its maximum value and then fluctuated. It can be inferred that the release and oxidation of char N were the primary causes of the final NO_x formation. The conversion of char N to NO_x is highly complex and may involve the release of CN, which is then converted to NO (Eqs. (23) and (24)). In this experiment, the non-counterflow structure of the oxidation zone nozzle (Fig. 2) suppressed the combustion intensity in the oxidation zone, reduced the radial temperature peak, and thereby inhibited the conversion of char N to NO_x [21].

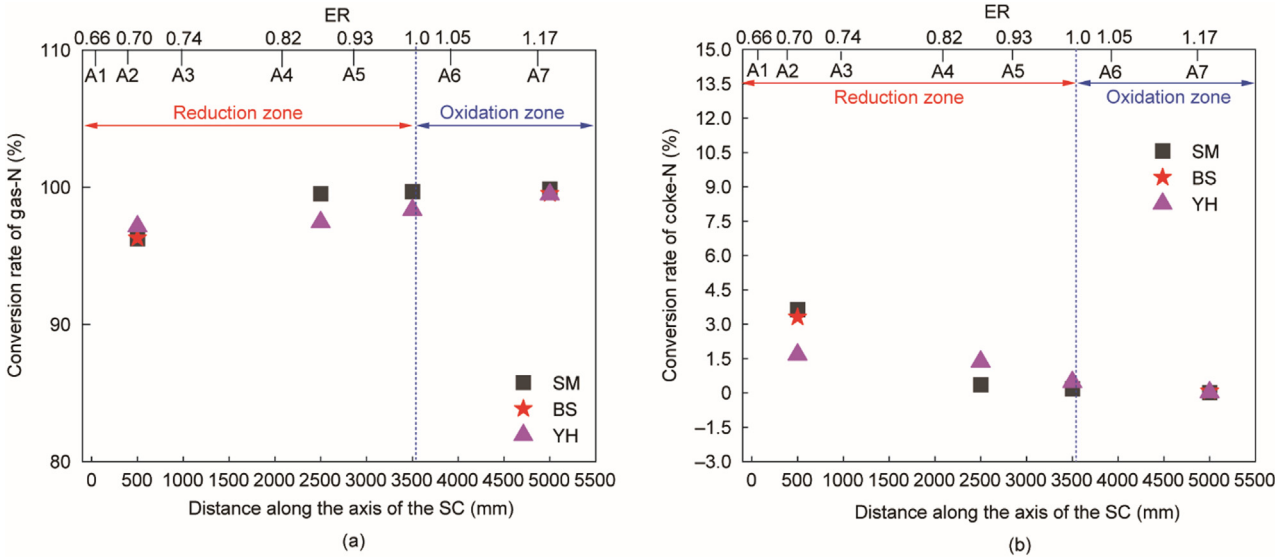

Fig. 25. The conversion rate of (a) gas phase N and (b) char N along SC.

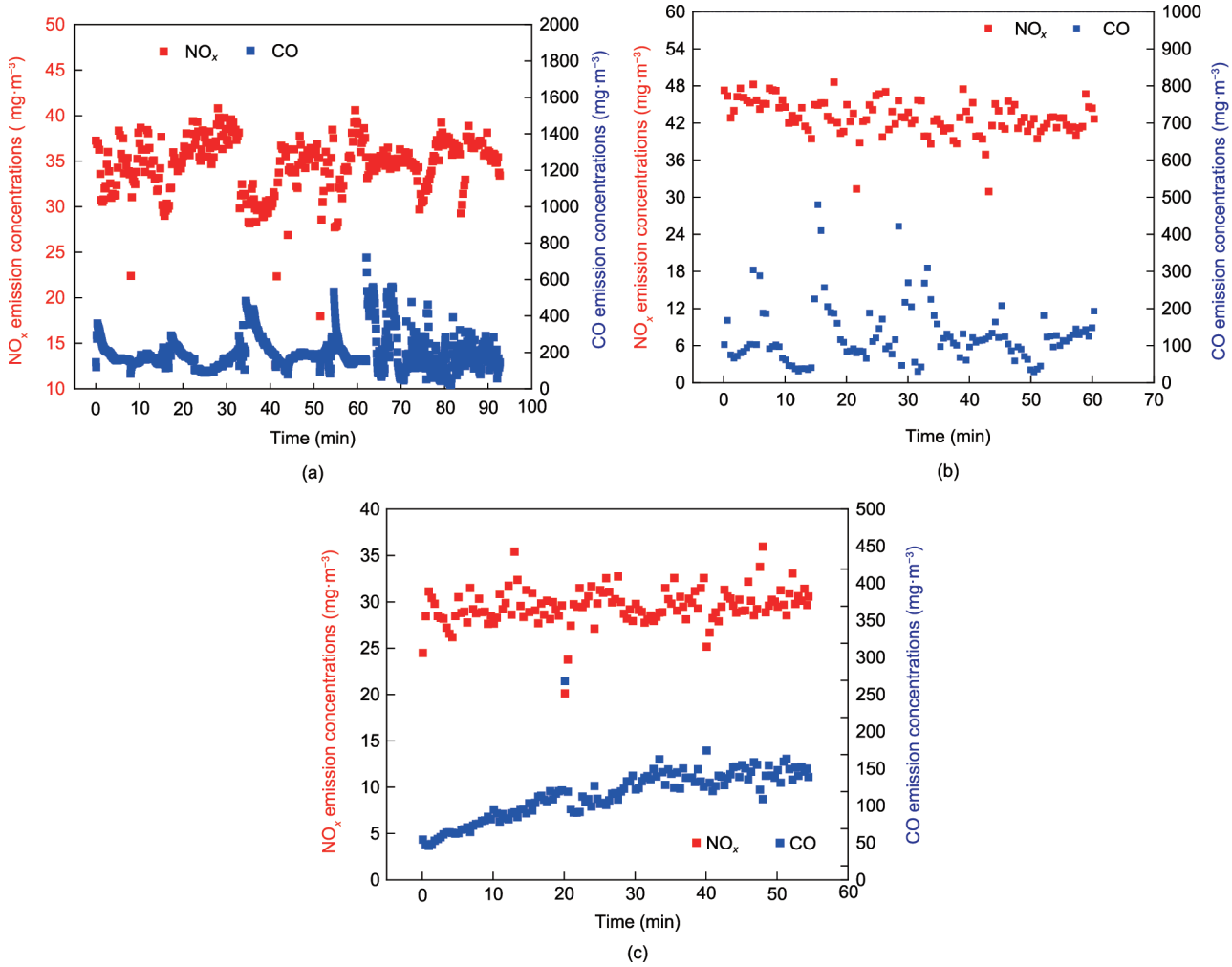

Fig. 26. The original NO_x and CO emissions of three types of coal purification-combustion: (a) SM, (b) BS, and (c) YH.

$$Chi + NO \leftrightarrow HCN + \cdots \quad (20)$$

$$CO + NO \leftrightarrow CO_2 + N_2 \quad (21)$$

$$NO + Cf \rightarrow C(O) + 1/2N_2 \quad (22)$$

$$O2 + (-C) \rightarrow (-CO) + (-CNO) \quad (23)$$

$$(-CNO) \rightarrow NO + (-C) \quad (24)$$

Figs. 25(a) and (b) show the conversion rates of coal N to gas-phase N and char N in the axial direction of the SC after air injection for the three types of coal. As air was gradually injected, the proportion of gas-phase N increased, whereas the proportion of char N decreased, further indicating that the combustion process of char was accompanied by the release and conversion of char N. The gas-phase N conversion rate at the outlet of the SC reduction zone reached 99.7%, an increase of 2%–3% compared to the inlet, indicating that the construction of the SC reduction zone facilitated the release and conversion of more char N to N_2. This also reduced the proportion of char N entering the oxidation zone, with only 0.2%–0.9% of coal N ultimately converted to NO_x in the oxidation zone.

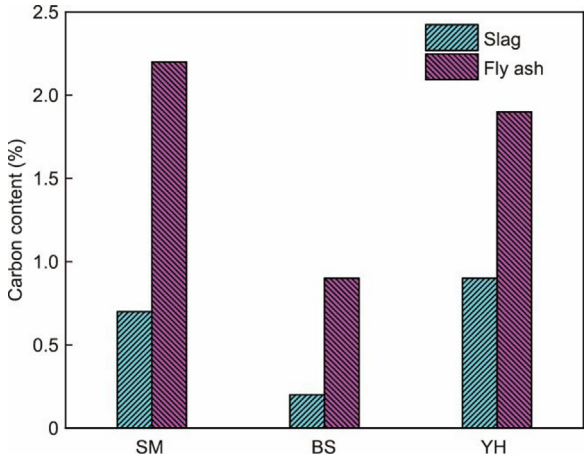

Fig. 27. The carbon content in slag and fly ash.

Fig. 26 presents the continuous emission concentrations of CO and NO_x (@6% O_2) at the SC outlet for the three types of coal. The average NO_x emission concentrations are 34.6 mg·m^{-3} for SM, 42.1 mg·m^{-3} for BS, and 28.4 mg·m^{-3} for YH, with average CO emissions below 200 mg·m^{-3}. The carbon content in the slag and fly ash is shown in Fig. 27, where the carbon contents were all below 2.5%, and the combustion efficiencies were 99.6%, 99.7%, and 99.7%, respectively, achieving efficient ultralow-nitrogen combustion of multiple coal types under low-load conditions. According to the results of Li et al. [48], fuel-type NO_x is suppressed under MILD combustion conditions, resulting in a reduction of approximately 40% in the total NO_x emissions compared to traditional combustion modes. Schaffel et al. [49] noted that in pulverized coal MILD combustion, the volatiles in coal are already in a high-temperature region with a low oxygen volume fraction before release, leading to a significant proportion of fuel nitrogen being converted to N_2. Additionally, the prolonged combustion process under low-oxygen and high-temperature conditions facilitated NO re-reduction reactions, further reducing the NO_x volume fraction. The nitrogen release and transformation pathways during the entire purification-combustion process are shown in Fig. 28 [5,9,17,42,50].

Fig. 29 shows a schematic of the complete purification-combustion process. The purification-combustion process can achieve efficient ultra-low nitrogen combustion of multiple coal types under 55% low-load conditions through the following mechanisms. First, the medium-temperature activation process converts coal particles into coal gas and highly active char, with 43.8%–53.1% of coal nitrogen being converted to N_2. Second, the high-temperature purification process effectively separates carbon and inorganic components, converting coal particles into a gas-phase fuel primarily composed of CO and H_2, which is conducive to stable combustion under low-load conditions, achieving a 96.6% reduction of coal nitrogen to N_2. Finally, the staged injection of oxidants and thorough mixing with gas-phase fuel reduce the combustion intensity and peak temperatures, achieving MILD combustion and inhibiting the oxidation of char nitrogen to NO_x during burnout. Therefore, compared with traditional gasification and combustion technologies, the purification-combustion technology demonstrates distinct advantages in reaction pathway optimization, fuel nitrogen control, inorganic matter removal, and operational stability under low-load conditions.

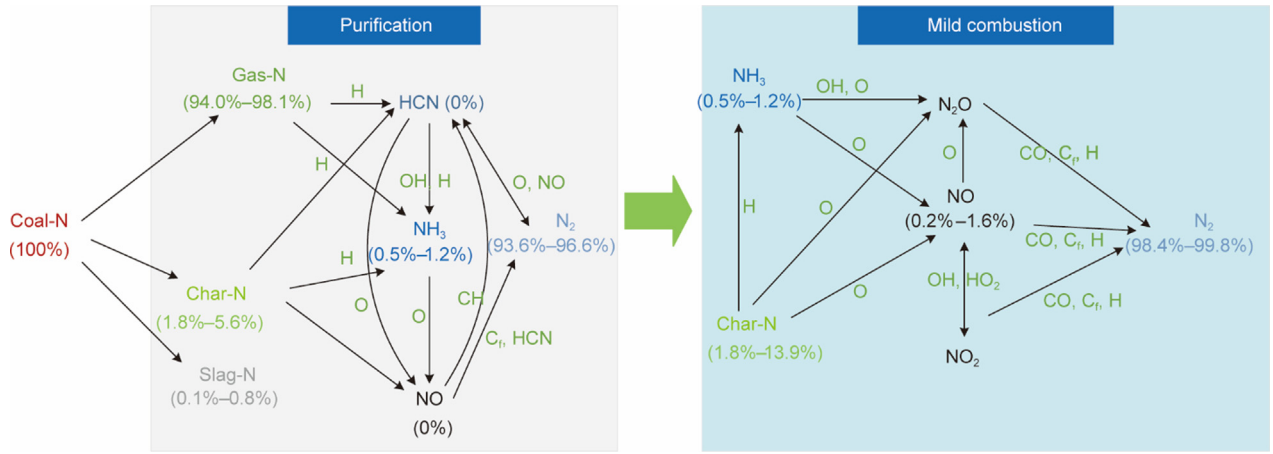

Fig. 28. Coal-N precipitation transformation path.

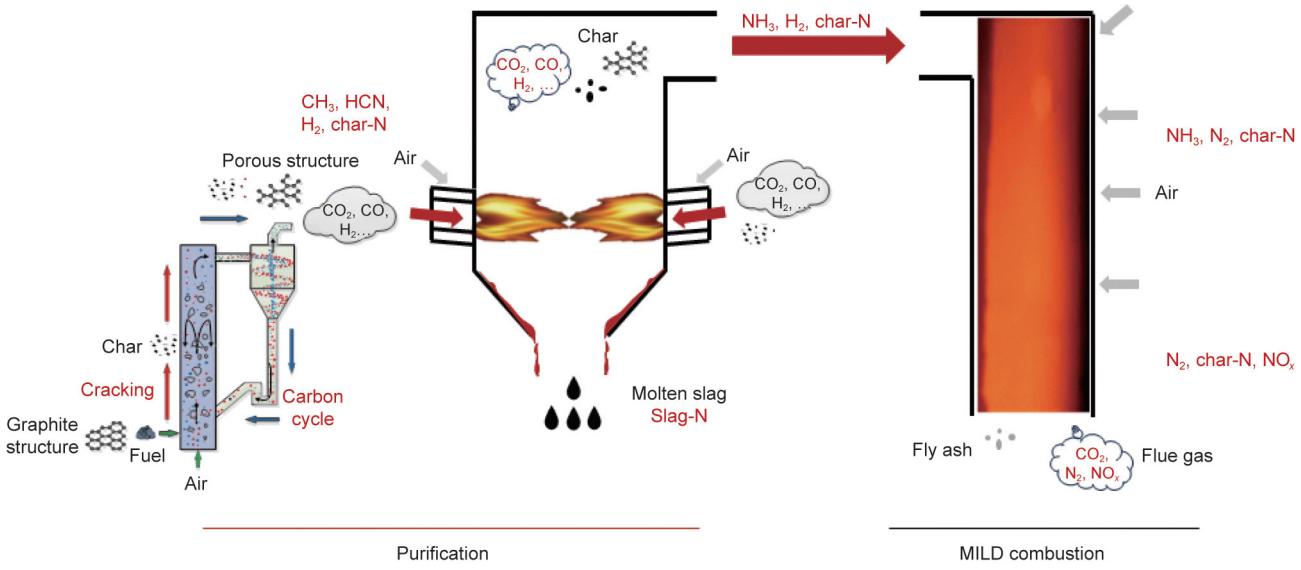

Fig. 29. Purification-combustion process diagram.

4. Conclusions

This study proposes an innovative concept of coal purification-combustion and verifies its feasibility and coal adaptability in a 200 kW purification-combustion device. The purification-combustion characteristics, nitrogen migration, and transformation characteristics of the three types of coal under low-load conditions were investigated. The main conclusions are as follows.

First, the medium-temperature activation process of coal primarily involves the release of volatile nitrogen and its reduction to N_2, with a conversion rate of coal nitrogen to N_2 reaching 43.8%–53.1%. During this process, coal particles are activated, which significantly increases the specific surface area of the char, fully develops the pore structure, and increases the number of active sites, which is conducive to high-temperature gasification reactions under low-load conditions.

Second, during the high-temperature purification process, 62%–85% of the inorganic components are separated, effectively achieving the separation of carbon and inorganic components. Coal particles are converted into high-temperature gas-phase fuel primarily composed of CO and H_2, and the pore structure of the char is further developed, which is beneficial for stable combustion under low-load conditions. The high-temperature purification process mainly involves the release of char nitrogen and its reduction to N_2, with the conversion rate of coal nitrogen to N_2 increasing to 93.6%–96.6%.

Additionally, the fuel primarily composed of high-temperature CO and H_2 achieved a MILD combustion process. In the reduction zone of the combustion furnace, NH_3 was completely converted to N_2, and char nitrogen was gradually released and reduced to N_2; the conversion rate of coal nitrogen to N_2 in the reduction zone increased to 99.6%. The oxidation zone is the burnout process of char, which mainly involves the release of char nitrogen and its oxidation to NO_x.

Finally, under low-load conditions, the original NO_x emissions at the furnace outlet are 34.6 $mg{\cdot}m^{-3}$ for SM, 42.1 $mg{\cdot}m^{-3}$ for BS, and 28.5 $mg{\cdot}m^{-3}$ for YH, with combustion efficiencies all above 99.6%, achieving efficient ultra-low nitrogen combustion of multiple coal types under low-load conditions.

CRediT authorship contribution statement

Shaobo Yang: Resources, Investigation, Data curation. **Shaobo Han:** Resources, Investigation, Data curation. **Ruifang Cui:** Investigation, Data curation. **Linxuan Li:** Investigation, Data curation. **Chen Liang:** Investigation. **Shuai Guo:** Investigation. **Neng Fang:** Investigation. **Wei Li:** Writing – review & editing, Investigation. **Qiangqiang Ren:** Writing – review & editing, Supervision, Project administration, Funding acquisition.

Declaration of competing interest

The authors declare that they have no known competing financial interests or personal relationships that could have appeared to influence the work reported in this paper.

Acknowledgments

This work was financially supported by the Chinese Academy of Sciences (CAS) Project for Young Scientists in Basic Research (YSBR-028).

References

[1] Lyu Q, Chai Z. Highly efficient and clean utilization of fossil energy under carbon peak and neutrality targets. Bulle Chin Acad Sci 2022;37(4):541–8.
[2] Jiang X, Yang H, Liu H, Zheng C, Liu D. Analysis of the effect of coal powder granularity on combustion characteristics by thermogravimetry. Proc CSEE 2002;22(12):142–5. Chinese.
[3] Li Q, Zhao C. Investigation on characteristics of pulverized coal combustion in O_2/CO_2 mixtures. Proc CSEE 2007;27(35):39–43. Chinese.
[4] Zheng C, Zhao Y, Guo X. Research and development of oxy-fuel combustion in China. Proc CSEE 2014;34(23):3856–64. Chinese.
[5] Glarborg P, Jensen AD, Johnsson JE. Fuel nitrogen conversion in solid fuel fired systems. Pror Energy Combust Sci 2003;29(2):89–113.
[6] Zhang X, Chen Z, Zhang M, Zeng L, Li Z. Combustion stability, burnout and NO_x emissions of the 300-MW down-fired boiler with bituminous coal: load variation and low-load comparison with anthracite. Fuel 2021;295:120641.
[7] Wang J, Fan W, Li Y, Xiao M, Wang K, Peng R. The effect of air staged combustion on NO_x emissions in dried lignite combustion. Energy 2012;37(1):725–36.
[8] Liu Y, Zhao Y, Zhang L, Wu J, Feng J, Zhou C, et al. Experiment and numerical study on combustion characteristics of low-nitrogen burners. Fuel 2023;351:128814.

[9] Tang H, Liu Z, Han X, Shen X, Liu Y, Wang S, et al. Experimental study on combustion characteristics of a 40 MW pulverized coal boiler based on a new low NO_x burner with preheating function. Energy 2024;305:132319.
[10] Wang Q, Chen Z, Han H, Zeng L, Li Z. Experimental characterization of anthracite combustion and NO_x emission for a 300-MWe down-fired boiler with a novel combustion system: influence of primary and vent air distributions. Appl Energy 2019;238:1551–62.
[11] Liu C, Hui S, Pan S, Zhou H, Zhang G, Wang D. Experimental investigation on NO_x reduction potential of gas-fired coal preheating technology. Energy Fuels 2014;28(9):6089–97.
[12] Lyu Q, Zhu S, Zhu J, Ouyang Z. Research and development on preheating combustion of pulverized coal. Proc CSEE 2022;42(18):6535–47. Chinese.
[13] Ouyang Z, Zhu J, Lyu Q. Experimental study on preheating and combustion characteristics of pulverized anthracite coal. Fuel 2013;113:122–7.
[14] Liu J, Liu Y, Zhu J, Ouyang Z, Man C, Zhu S, et al. Bituminous coal deep regulated ultra-low NO_x flameless combustion with fluidized self-preheating fuel: a 2 MWth experimental study. Fuel 2021;294:120549.
[15] Zhu S, Hui J, Lyu Q, Ouyang Z, Zeng X, Zhu J, et al. Experimental study on pulverized coal swirl-opposed combustion preheated by a circulating fluidized bed. Part A. Wide-load operation and low-NO_x emission characteristics. Energy 2023;284:128573.
[16] Hui J, Zhu S, Lin J, Li Z, Cao X, Lyu Q. Nitrogen conversion characteristics of pulverized coal preheating combustion in wide load ranges. J Energy Inst 2024;116:101747.
[17] Wang X, Zhou B, Wang Y, Bukhsh K, Wang X, Tan H. Nitrogen migration and gasification characteristics of pulverized coal using the novel gasification-combustion technology. J Clean Prod 2024;479:143984.
[18] Yang S, Ren Q, Han S, Cui R, Hu Y, Heng Y, et al. Coal gasification-combustion system—part I: principle and nitrogen migration characteristics. Fuel 2025;398:135527.
[19] Hu Y, Li W, Yang S, Han S, Cui R, Zhang C, et al. Experimental study on migration and transformation of inorganic components during purification-combustion. Chem Eng J 2024;500:156917.
[20] Han S, Ren Q, Yang S, Cui R, Hu Y. Characteristics of coal purification combustion and wide-load NO_x emissions on a 200 kW platform. J China Coal Soc 2024;49(10):4060–70. Chinese.
[21] Su K, Ouyang Z, Wang H, Ding H, Zhang J, Wang W. Effects of activated fuel and staged secondary air distributions on purification, combustion and NO_x emission characteristics of pulverized coal with purification-combustion technology. Energy 2024;302:131883.
[22] Su K, Ouyang Z, Wang W, Ding H, Zhang J, Wei C, et al. Experimental study on effects of premixed air distribution on preheating combustion characteristics and NO_x emission of pulverized coal. Fuel 2023;344:128076.
[23] Han S, Ren Q, Yang S, Cui R, Hu Y, Zhang C. A novel coal purification-combustion system: purification and combustion characteristics. Energy 2025;323:135897.
[24] Xiao Y, Song G, Song W, Yang Z, Lyu Q. Influence of feeding position and post-combustion air arrangement on NO_x emission from circulating fluidized bed combustion with post-combustion. Fuel 2020;269:117394.
[25] Liang C, Li W, Wang W, Zhou L, Guo S, Ren Q. Experimental investigation on thermal modification and burnout of residual carbon in coal gasification fine slag. Energy 2024;295:131162.
[26] Wang X, Zhou B, Xu S, Liu G, Wang Y, Xiong X, et al. Numerical analysis of coal size influencing the performance and slag flow characteristics of gasifier based on a comprehensive model. Fuel 2023;332:125934.
[27] Xie T, Wang H. Opposed jet burner and Tsuji burner for representative laminar flamelet with differential molecular diffusion for non-premixed combustion modeling. Combust Flame 2024;264:113428.
[28] Guo S, Liang C, Chen Z, Li W, Ren Q. A pilot scale test on the fluidized melting combustion of coal gasification fine slag. Waste Manag 2024;190:593–9.
[29] Su K, Ouyang Z, Wang H, Zhang J, Ding H, Wang W. Research on purification, combustion and NO_x emission characteristics of pulverized coal preheated by a novel self-sustained purifying burner. Fuel 2024;366:131436.
[30] Wu Y, Liu S, Chen Y, Yang Y, Yang H. Alkali and alkaline earth metals catalytic steam gasification of ashless lignin: influence of the catalyst type and loading amount. Fuel 2024;356:129549.
[31] Liu G, Benyou P, Benfell KE, Bryant GW, Tate AG, Boyd RK, et al. The porous structure of bituminous coal chars and its influence on combustion and gasification under chemically controlled conditions. Fuel 2000;79(6):617–26.
[32] Xu J, Tang H, Su S, Liu J, Xu K, Qian K, et al. A study of the relationships between coal structures and combustion characteristics: the insights from micro-Raman spectroscopy based on 32 kinds of Chinese coals. Appl Energy 2018;212:46–56.
[33] Zhang Y, Zhu J, Lyu Q, Pan F, Zhu S. Characteristics of preheating combustion of power coal with high coking properties. J Therm Sci 2020;30(4):1108–15.
[34] Vargas S, Frandsen FJ, Dam-Johansen K. Rheological properties of high-temperature melts of coal ashes and other silicates. Pror Energy Combust Sci 2001;27(3):237–429.
[35] Lin X, Liu J, Ideta K, Miyawaki J, Wang Y, Mochida I, et al. Cation induced microstructure and viscosity variation of molten synthetic slag analyzed by solid-state NMR. Fuel 2020;267:117310.
[36] Zhou L, Ren Q, Cui R, Li W. Experiment on preparation of porous glass-ceramics by inorganic gel casting from coal-based slag. Constr Build Mater 2023;394:132222.
[37] Su K, Ding H, Ouyang Z, Zhang J, Zhu S. Experimental study on effects of multistage reactant and air jet velocities on self-preheating characteristics and NO_x emission of burning pulverized coal. Fuel 2022;325:124879.
[38] Smoot LD, Smith P. Coal combustion and gasification. Berlin: Springer Chemical Engineering; 1985.
[39] Haynes BS. Reactions of ammonia and nitric oxide in the burnt gases of fuel-rich hydrocarbon-air flames. Combust Flame 1977;28:81–91.
[40] Zhu J, Ouyang Z, Lyu Q. An experimental study on NO_x emissions in combustion of pulverized coal preheated in a circulating fluidized bed. Energy Fuels 2013;27(12):7724–9.
[41] Liu Y, Liu J, Lyu Q, Zhu J, Pan F. Microstructure analysis of fluidized preheating pulverized coal under O_2/CO_2 atmospheres. Fuel 2021;292:120386.
[42] Kambara S, Takarada T, Toyoshima M, Kato K. Relation between functional forms of coal nitrogen and NO_x emissions from pulverized coal combustion. Fuel 1995;74(9):1247–53.
[43] Weber R, Smart JP, Kamp WV. On the (MILD) combustion of gaseous, liquid, and solid fuels in high temperature pre-heated air. Prog Energ Combust 2005;30(2):2623–9.
[44] Liu W, Ouyang Z, Cao X, Na Y. Experimental research on flameless combustion with coal preheating technology. Energy Fuel 2018;32(6):7132–41.
[45] Zhang H, Yue G, Lu J, Jia Z, Mao J, Fujimori T, et al. Development of high temperature air combustion technology in pulverized fossil fuel fired boilers. Proc Combust Inst 2007;31(2):2779–85.
[46] Cavaliere A, De Joannon M. Mild combustion. Pror Energy Combust Sci 2004;30(4):329–66.
[47] Kumar S, Paul PJ, Mukunda HS. Studies on a new high intensity low-emission burner. Proc Combust Inst 2002;29(1):1131–7.
[48] Li P, Wang F, Tu Y, Mei Z, Zhang J, Zheng Y, et al. Moderate or intense low-oxygen dilution oxy-combustion characteristics of light oil and pulverized coal in a pilot-scale furnace. Energy Fuels 2014;28(2):1524–35.
[49] Schaffel N, Mancini M, Szle A, Weber R. Mathematical modeling of MILD combustion of pulverized coal. Combust Flame 2009;156(9):1771–84.
[50] Su K, Ding H, Ouyang Z, Zhang J, Zhu S. Effects of interaction between axial and radial secondary air and reductive intensity in reduction region on combustion characteristics and NO_x emission of coal preheated by a self-preheating burner. J Therm Sci 2024;33(1):249–67.